การปรับตัวของเชื้ออไวรัสพิษสุนัขบ้าในเซลล์ที่มีต้นกำเนิดไม่ใช่ระบบประสาท
โดยเชื้ออมีความรุนแรงขึ้น**และ**ศึกษาระดับยีนควบคุม

นางสาวพัทธมน วิโรจนาภิรมย์

วิทยานิพนธ์นี้เป็นส่วนหนึ่งของการศึกษาตามหลักสูตรปริญญาวิทยาศาสตรดุษฎีบัณฑิต
สาขาวิชาชีวเวชศาสตร์ (สหสาขาวิชา)
บัณฑิตวิทยาลัย จุฬาลงกรณ์มหาวิทยาลัย
ปีการศึกษา 2554
ลิขสิทธิ์ของจุฬาลงกรณ์มหาวิทยาลัย

BHK-CELL ADAPTED CANINE RABIES VIRUS VARIANT: MUTATION IN INTERGENIC

PHOSPHOPROTEIN AND MATRIX PROTEIN GENE NON-CODING REGION MAY

CONFER HIGHER NEUROVIRULENCE IN ADULT MICE

MISS PHATTHAMON VIROJANAPIROM

A Thesis Submitted in Partial Fulfillment of the Requirements

for the Degree of Doctoral of Philosophy Program in Biomedical Sciences

(Interdisciplinary Program)

Graduate School

Chulalongkorn University

Academic Year 2011

พัทธมน วิโรจนาภิรมย์ : การปรับตัวของเชื้ออไวรัสพิษสุนัขบ้าในเซลล์ที่มีต้นกำเนิดไม่ใช่ระบบ
ประสาทโดยเชื้ออมีความรุนแรงขึ้นการศึกษาระดับยีนควบคุม (BHK-CELL ADAPTED
CANINE RABIES VIRUS VARIANT: MUTATION IN INTERGENIC PHOSPHOPROTEIN
AND MATRIX PROTEIN GENE NON-CODING REGION MAY CONFER HIGHER
NEUROVIRULENCE IN ADULT MICE) อ. ที่ปรึกษาวิทยานิพนธ์หลัก: ศ.นพ.ธีระวัฒน์
เหมะจุฑา, อ. ที่ปรึกษาวิทยานิพนธ์ร่วม: ดร.ผกามาศ ขาวปลอด, 81 หน้า.

ความสามารถในการก่อโรคของเชื้ออไวรัสโรคพิษสุนัขบ้าโดยทั่วไปสามารถถูกทำให้
ลดลงได้โดยการเลี้ยงเชื้ออไวรัสโรคพิษสุนัขบ้าในเซลล์ที่มีกำเนิดมาจากเซลล์นอกระบบ
ประสาทหรือโดยการปรับเปลี่ยนทางพันธุกรรม ในทางตรงกันข้ามเมื่ออทำการเลี้ยงเชื้ออไวรัส
โรคพิษสุนัขบ้าที่ได้จากสุนัขไทยที่ตายจากการเป็นโรคพิษสุนัขบ้า (QS-05) ในเซลล์ไตของ
ลูกหนูแฮมสเตอร์ (baby hamster kidney, BHK-21) กลับทำให้เชื้ออไวรัสโรคพิษสุนัขบ้าใหม่ที่
ได้นี้นมีความสามารถในการก่อโรคสูงขึ้นภายหลังจากการเลี้ยงเชื้ออไวรัสโรคพิษสุนัขบ้า QS-
05 7 ครั้งในเซลล์ไตของลูกหนูแฮมสเตอร์ (QS-BHK-P7) เชื้ออไวรัสดังกล่าวมีความสามารถใน
การทำให้หนูทดลองตายจากการฉีดเชื้ออไวรัสโรคพิษสุนัขบ้าทั้งทางกล้ามเนื้ออและทางสมอง
โดยตรง ในขณะที่ QS-05 สามารถทำให้หนูทดลองตายได้เฉพาะเมื่ออฉีดเชื้ออไวรัสโรคพิษสุนัข
บ้าทางสมองเท่านั้น เมื่ออทำการเปรียบเทียบลำดับเบสทั้งงหมดของ QS-05 และ QS-BHK-P7
พบว่ามีการการกลายพันธุ์ซึ่งงเป็นแบบ missense mutation 3 ตำแหน่ง พบในส่วน
ectodomain ของยีนไกลโคโปรตีน (S23R ซึ่งงเป็นตัวบ่งชี้ถึงการปรับตัวในเซลล์นอกระบบ
ประสาทและ H424P ซึ่งงไม่อยู่ในส่วนของ PDZ ที่เป็นตัวบ่งชี้ถึงความรุนแรงของเชื้ออไวรัสโรค
พิษสุนัขบ้า) และอีกตำแหน่งพบในยีนโพลีเมอเรส (I1711V) นอกจากนี้ยังพบการกลายพันธุ์
แบบ point mutation อีกตำแหน่งที่ adenine ตำแหน่งที่ 7 ของ polyadenylation signal
ระหว่างยีนฟอสโฟโปรตีนและยีนแมตทริคโปรตีน โดยบทบาทของการกลายพันธุ์ในยีนโพลี
เมอเรสและส่วนระหว่างยีนฟอสโฟโปรตีนและยีนแมตทริคโปรตีนยังคงต้องทำการศึกษาต่อไป

สาขาวิชาชีวเวชศาสตร์............................. ลายมือชื่ออนิสิต ....
ปีการศึกษา 2554 .... ลายมือชื่ออ.ที่ปรึกษาวิทยานิพนธ์หลัก.................
ลายมือชื่อ อ.ที่ปรึกษาวิทยานิพนธ์ร่วม ....

4989681020 : MAJOR   BIOMEDICAL SCIENCES

KEYWORDS : non-neuronal passage / polyadenylation signal / rabies virus / virulence / non-coding region

PHATTHAMON VIROJANAPIROM: BHK-CELL ADAPTED CANINE RABIES VIRUS VARIANT: MUTATION IN INTERGENIC PHOSPHOPROTEIN AND MATRIX PROTEIN GENE NON-CODING REGION MAY CONFER HIGHER NEUROVIRULENCE IN ADULT MICE. ADVISOR: PROF.THIRAVAT HEMACHUDHA, M.D., CO-ADVISOR: PAKAMATZ KHAWPLOD, Ph.D., 81 pp.

Attenuation of rabies virus can be achieved by passaging virus into non-neuronal cells or by modification of genetic element(s). Following serial passages of Thai canine street rabies virus, QS-05, into BHK-21 cells, gave rise to highly pathogenic virus. At seventh passage, QS-BHK-P7 virus was able to cause lethality in adult mice by peripheral intramuscular and intracerebral (IC) challenges whereas its parental isolate could only kill by IC route. Comparison of whole genome sequences revealed that there were three missense mutations, two were located in ectodomain region of glycoprotein (G) gene (non-neuronal marker S23R and H424P at non-PDZ or pathogenic/immunogenic determinant sites) and the other (I1711V) in polymerase (L) gene. Another point mutation was at the seventh adenine residue of the poly (A) signal residing between the phospho (P) and matrix (M) protein genes. Roles of such mutation in L and intergenic P-M region remain to be elucidated.

Field of Study : Biomedical Sciences   Student's Signature _____

Academic Year : 2011 _____   Advisor's Signature _____

Co-advisor's Signature _____

ACKNOWLEDGEMENTS

CONTENTS

Chapter

LIST OF TABLES

LIST OF FIGURES

LIST OF ABBREVIATIONS

AUAP   abridged Universal Amplification Primer

BHK   baby hamster kidney

CAT   chloramphenicol acetyltransferase

CEF   chicken embryo fibroblast

CNS   central nervous system

CPE   cytopathic effect

C-terminus   carboxy terminus

CVS   challenge virus standard

ERA   Evelyn-Rokitnicki-Abelseth

ESCRT   endosomal sorting complex required for transport

G   glycoprotein

GSP   gene-specific primer

HEP-Flury   high-egg-passage Flury

HmLu   hamster lung

IC   intracerebral

IF   immunofluorescent

IFN   interferon

IGR   intergenic region

IM   intramuscular

IPTG   isopropyl thiogalactoside

IRF-3   interferon regulatory factor 3

L   polymerase

LC8   cytoplasmic dynein light chain

Le   leader

LD50   median lethal dose

M	matrix protein
MAST	microtubule-associated serine/threonine-protein kinase
N	nucleoprotein
NA	neuroblastoma
NC	nucleocapsid
NCR	non-coding region
Nedd4	neural precursor cell expressed developmentally down-regulated protein4
NES	nuclear export signal
NLS	nuclear export signal
N-terminus	amino terminus
P	phosphoprotein
PCR	polymerase chain reaction
PD-1	programmed death 1

PDZ-BS   PDZ binding site

pi   post infection

PTPN4   non-receptor protein tyrosine phosphatase 4

RdRp   RNA-dependent RNA polymerase

RI   replicative intermediate

RIG   retinoic acid-inducible gene

RNP   ribonucleoprotein

RV   rabies virus

SAD   Street-Albama-Dufferin

SHBRV   silver-haired bat-associated rabies virus

SMB   suckling mouse brain

STAT   signal transducers and activators of transcription

Tr   trailer

UTR   untranslated region

VSV   vesicular stomatitis virus

WGS   whole genome sequence

CHAPTER I

INTRODUCTION

1. Background and Rationale

Rabies virus (RV) is a non-segmented negative-stranded RNA virus. It belongs to

order *Mononegavirales*, family *Rhabdoviridae*, genus *Lyssavirus* (Albertini et al., 2011).

RV is a neurotropic virus, causing an almost invariably fatal encephalomyelitis. It infects

animals mainly through bites contaminated with RV containing saliva. Once RV enters

the wound, it multiplies at muscle cells, then travels to the central nervous system (CNS)

by retrograde axonal transport (Hemachudha et al., 2002).

Passage of RV obtained from dog brain in heterologous cell types, such as baby

hamster kidney (BHK-21) cells, results in the selection of geno- and pheno-typically

different variants from those mouse-brain passage viruses. The latter is more pathogenic

in adult mice than the BHK-cell passage variant, which grows faster in BHK cells (5).

QS-BHK-P7 is a variant obtained from 7 serial passages of QS-05 Thai canine

street RV isolated from a rabid dog brain into BHK-21 cells. This virus was developed at

Queen Saovabha Memorial Institute. QS-BHK-P7 had increased neurovirulence as

compared to QS-05. It was able to infect and cause death in adult mice by both

intracerebral (IC) and peripheral intramuscular (IM) challenges. Parental strain, QS-05, cause lethality in adult mice only by IC route.

Such finding is intriguing since rabies viral pathogenicity usually became attenuated following sub-passaging in non-neuronal cell line. One of the examples is SAD-B19 strain, the oral vaccine strain, which was established by several sub-passaging of SAD strain in BHK cells. This resulted to the attenuation of pathogenicity (Vos et al., 1999). CVS (challenge virus standard)-B2c, established by sub-passaging of CVS-24 in non-neuronal cells, contained S23R mutation in glycoprotein (G). Higher replication rate was observed in non-neuronal cells, despite the fact that this strain was less neurotropic both in *in vitro* and *in vivo* comparing to CVS-N2c, neuronal passage of CVS-24 (Morimoto et al., 1998). This is predictable since virulence is inversely correlated to replication rate. Ni-CE strain, nonpathogenic strain, showed phenotypic differences from its parental strain, Nishigahara, after a hundred passages following IC inoculation (Mita et al., 2008). It has been hypothesized that the increased virulence of BHK-adapted strain following peripheral inoculation is due to the adaptation or modification of G to better facilitate the spread of the virus.

In this study, we here reported the phenotypic differences as examined in neuroblastoma (NA) cells between QS-05 and its non-neuronal passage, QS-BHK-P7. Greater number and larger size of viral particles as well as degree of foci formation were demonstrated in the case of QS-BHK-P7 as compared to its parental virus. Increased

pathogenicity was clearly demonstrated in adult mice by both IM and IC challenges at differnt virus inoculums. Aligned sequences of these 2 viruses were compared. Based on the results of whole genome sequencing, genetic alterations were found located at polyadenylation signal between P and M intergenic region (IGR) as well as at G (2 missense mutations) and L (one missense mutation). The significance of these mutations was discussed with the possible role of mutations at IGR non-coding region and at L gene in determining neurovirulence and pathogenicity.

2. Research Question

Does adaptation of street rabies virus in non-neuronal cells confer the difference in pathogenicity?

At which location(s) of the gene segment(s) of non-neuronal passage virus can be found altered and which one(s) of them could be responsible for increasing pathogenicity?

3. Objective of the Study

To study the impact of viral adaptation in non-neuronal cells on viral pathogenicity

To study the genetic differences between parental virus and its non-neuronal passage

4. Hypothesis

It is possible that adaptation of street rabies virus passage in non-neuronal cells can better facilitate spread to CNS

5. Key Words

rabies virus, non-neuronal passage, virulence, polyadenylation signal, non-coding region

6. Expected Benefits and Applications

The results of this study may emphasize the role of noncoding region such as, intergenic region of RV in determining pathogenicity.

CHAPTER II

REVIEW OF RELATED LITERATURES

Review of Related Literatures

1. Genome organization, Replication and Transcription

Rabies virus (RV), non-segmented negative-stranded RNA virus, belongs to the order mononegavirales, family Rhabdoviridae, genus *Lyssavirus*. Its particle is approximately 180x75 nm with 75-nm in diameter and 100-300 nm in length. Its genome consists of 11923 or 11928 nucleotides, containing a leader (Le) sequence at the 3' end, followed by 5 monocistronic genes that encode the nucleoprotein (N), phosphoprotein (P), matrix protein (M), glycoprotein (G) and large protein (L) and trailer (Tr) sequences at the 5' end of the viral genomic RNA, 3'-Le-N-P-M-G-L-Tr-5'. At the center of the bullet-shaped virus particle is a core of helical RNA, ribonucleoprotein (RNP), surrounded by a lipid-protein envelope. RNP core, an active transcription/replication complex, consists of single-stranded genome RNA encapsidated with N, polymerase cofactor P and virion-associated RNA-dependent RNA polymerase (RdRp) L (figure 1) (Wunner, 2007). RV is a neurotropic virus causing fatal neurological disease. It infects animals mainly through bites contaminated with saliva containing the virus. Once RV enters the wound, it multiplies at muscle cells then travels from periphery, site of infection, to CNS by retrograde axonal transport (Hemachudha et al., 2002). The virus enters cells through

coated pits or via cell surface receptors, mediated by viral G fusing with the cellular membrane. Then viral G mediates low-pH-dependent fusion with the endosomal membrane and the virus is uncoated resulting in the release of helical nucleocapsid (NC). The 5 structural genes of the genome RNA are transcribed into 5 positive-strand mRNA and a full-length positive-strand (antigenome) replicative intermediate (RI) RNA, which serves as template for replication of progeny genome (negative-strand) RNA. The N, P, M and L proteins are synthesized from their respective mRNAs on the free ribosomes in the cytoplasm. G protein is synthesized from G-mRNA on membrane-bound ribosomes. After progeny genome RNA is encapsidated by N, P and L protein to form RNP structures, M protein binds to the RNP and condenses into the bullet-shaped structures. They then interact with trimeric G proteins anchored in the plasma membrane and assemble into virus particles that bud out of infected cell (figure 2) (Albertini et al., 2011 and Okumura et al., 2011).
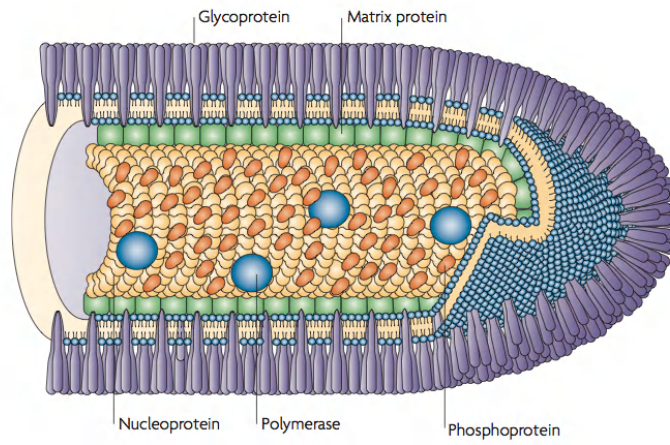
Figure 1 Structure of rabies virus (Schnell et al., 2010)
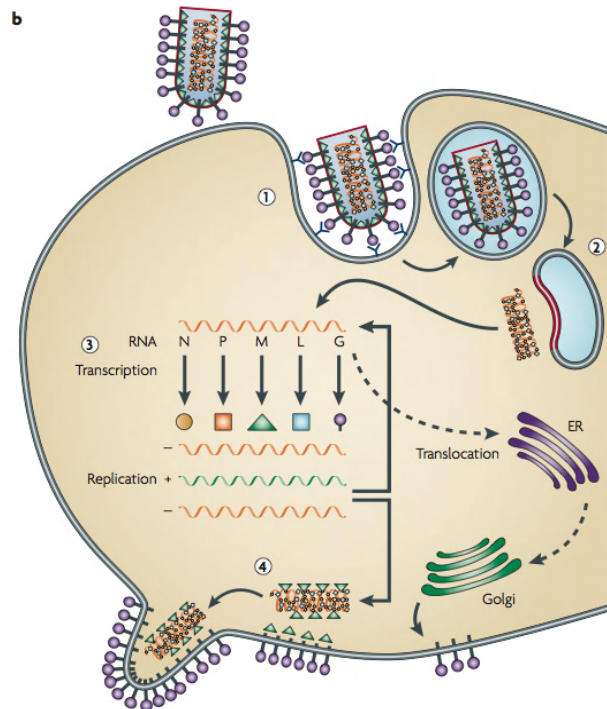
Figure 2 Rabies virus replication and transcription (Schnell et al., 2010)

2. Pathogenicity of rabies virus

2.1 Nucleoprotein

The encapsidation of viral genomic RNA as well as mRNAs by N protein is critical for protecting them from cellular degradation. Moreover, the polymerase complex of non-segmented negative-stranded RNA virus recognizes only N protein-encapsidated viral genome. With the help of P, N protein can specifically bind to its templates. The ratio of N and P protein is approximately 2:1, 1 monomer of P to 2 protomers of N (Albertini et al., 2011).

Phosphorylation of N protein at serine residue 389 has been demonstrated to be important for regulating viral transcription and replication. Minigenome of RV with mutation at this position from serine to another different charged or uncharged residues resulted to unphosphorylated N protein and decreased transcription and replication. With similar amount of N in transfected cells, mRNA transcripts were declined in unphosphorylated N mutants. Introduction of mutation at serine 389 into SAD-B19 full-length clone also resulted to the same outcome observed in minigenome system. Transcription, replication and viral titer of mutant RV were reduced while unphosphorylated N protein was detected. Phosphorylation of RV N protein might play role in regulating viral transcription/replication (Wu et al., 2002).

N protein was reported to involve in determining RV virulence. Switching of N gene between Nishigahara and Ni-CE strains resulted to 100% lethal infection following IC inoculation of this chimeric Ni-CE virus in adult mice (Shimizu et al., 2007).

N protein involves in host immune evasion. It plays significant role in evasion of RIG-I-mediated innate immunity. RIG-I, retinoic acid-inducible gene, consists of 2 domains, CARDS and DExD/H-box helicase domain. The former domain is responsible for RIG-I activation through binding to viral RNA. Type I interferon (IFN) expression is the consequence of this activation complex. N of Nishigahara strain has a potential to inhibit the activation of RIG-I, whereas Ni-CE strain cannot. Comparison of N protein between these strains showed that there were 3 different amino acids located at the C-terminal domain. By generating chimeric Ni-CE virus containing mutation(s) from Nishigahara strain, it has been shown that phenylalanine at position 273 and Tyrosine at position 394 of Nishigahara N gene are important for evasion of RIG-I-mediated interferon regulatory factor 3 (IRF-3) activation. This may explain how Nishigahara can be able to kill adult mice following IC inoculation (Masatani et al, 2010 and 2011).

2.2 Phosphoprotein

P protein is a cofactor in RdRp. The importance of P in virus replication was emphasized by the use of replication-defective RV with deletion of the entire P gene from high-egg-passage (HEP)-Flury strain. This P-deleted RV could not produce

progeny virus unless it was trans-supplemented with extra P in infected cells. It also lost the ability to cause lethal infection in both adult and suckling mice (Shoji et al., 2004).

Apart from being cofactor in RdRp during transcription and replication, P also functions as RV chaperone. The carboxy-terminus (C-terminus) end of P protein specifically binds to N-RNA complex, which served as template for viral transcription and replication. The first 19 amino acids residing at amino-terminus (N-terminus) end bind to polymerase in order to fix the polymerase to its template. Another function of P is to protect newly synthesized soluble N through binding with residue 4-40 of P. These residues have negatively charge that resembles RNA structure (Mavrakis et al., 2006).

The cayboxy-terminus end of P has binding site for cytoplasmic dynein light chain (LC8), which might involve in intracellular transport and might have impact on RV pathogenicity. However, recombinant SAD-B19 with deleted LC8-interacting motif did not alter the pathogenicity in mice after peripheral challenge. The recombinant virus with additional R333D mutation in G had decrease in mortality rate in suckling mice following IM inoculation (Mebatsion et al., 2001).

P plays role in evading/ suppressing host immune response. It consists of 3 nuclear transport signals, one nuclear localization signal (NLS) and two nuclear export signals (NES). NLS (located at amino acid position 172-297) functions during the steady state of infection, whereas NES plays role during the activated state of infection. It down-

regulates cellular antiviral response via the mechanism of P-STAT1 (signal transducers and activators of transcription 1) complex retention in the cytoplasm.The inhibition of STAT2 nuclear translocalization induced by IFN-alpha was observed following the binding of rabies P to STAT2 of infected cells. RV P also interferes with the IFN activation of infected cells by abolishing IRF-3 phosphorylation. P of attenuated Ni-CE strain has been shown to be more sensitive to IFN-alpha than Nishigahara strain. As a result of mutation at NES, less nuclear export of rabies P was observed. This resulted to ineffective inhibition of IFN-activated STAT1 nuclear translocalization (Brzozka et al., 2005 and 2006 and Ito et al., 2010).

Host immune response also plays role in viral pathogenesis. Up-regulation of immuno-inhibitory molecules; B7-H1, HLA-G and FasL, is observed in rabies-infected neurons. The exhaustion or death of T cells is the consequence of interaction between these ligands to the receptors expressing on T cells (Programmed Death 1; PD1, CD8 and Fas, respectively). This, in turn, results in immune evasion and invasion of nervous system (Lafon et al., 2008).

2.3 Matrix protein

M protein is a multi-functional protein. It plays role in regulating rabies transcription/replication, RNP condensation and viral budding.

RV M is the major component of viral assembly and budding, taking place at plasma membranes of infected host cells. It condenses the helical NC core into tightly coil shape, which then binds to RNP to form highly condensed skeleton-like structure. The N-terminus end of M gene contains many positively charged residues, which interact with negatively charged host membrane. This region also has the late domain that plays role in viral budding by interacting with host proteins. One of RV late domain, PPxY (amino acid residues 35-38 of M gene), interacts with host cell WW-domain called Nedd4 (neural precursor cell expressed developmentally down-regulated protein 4). The result of which is to recruit host proteins involved in endosomal sorting complex required for transport (ESCRT) pathway, normally found at endosomal membrane, to the budding site. Mutation at this region results to the defect in viral budding (Graham et al., 2008 and Okumura et al., 2011).

The evidence of function of RV M was demonstrated by the construction of M-deficient RV, SAD∆M. As compared to its wild-type recombinant virus, this mutant showed higher accumulation of G protein at the cell surface with a decrease in total infectious particles to 10,000-fold. This may reflect deficiency in virus formation. Moreover, 500,000-fold decrease in cell-free virions was observed in cells infected with this mutant. This may also imply defect in virus budding as the result of unsuccessful interaction between G and RNP which required specific binding of cytoplasmic tail of G protein to M-RNP (Mebatsion et al., 1999).

SADΔM exhibits higher expression of G protein on the surface of infected NA cells as compared to P-deleted mutant, SADΔP. This is due to the intactness of polymerase function. As a result, this mutant can induce humoral anti-RV-G in greater amount than the latter mutant. P-deleted mutant had deficiency in viral replication whereas M-deleted mutant replication was still possible but impaired (Cenna et al., 2009).

M also serves as regulator for transcription and replication of viral RNA by mediating the switch from mRNA synthesis to genomic RNA synthesis. This role is independent from its viral assembly function. Transcription rate (mRNA/genome) was lower in RV SAD-L16 transfected cells with over-expressed M protein as compared to transfected cells without extra M protein. Chimeric virus, SAD-LM, with attenuation of M expression by translocation of M to downstream of L gene, had increase in transcription rate, however, the replication was diminished as compared to the one with normal expression of M gene (Finke et al., 2003).

M may also involve in virulence of RV in adult mice. Generation of chimeric virus by replacing M gene of avirulent Ni-CE strain with virulent Nishigahara strain could cause lethal infection in adult mice following IC inoculation. This was evident despite the growth efficiency of this chimeric virus was lower than its wild-type recombinant Ni-CE virus (Shimizu et al., 2007).

Similar strategy has been applied to avirulent RC-HL strain by exchanging M gene of Nishigahara strain in the background of RC-HL strain. This chimeric virus did not revert to virulent phenotype (Yamada et al., 2006).

The cytopathogenicity of host cells was found to be inversely correlated with viral pathogenicity in experimental mouse model. NA cells infected with Nishigahara strain with mutation at position 95 of M gene, exhibited less cytopathic effect (CPE) than Ni-CE infected cells. The attenuation of M expression resulted in higher viral transcription rate and apoptosis of infected cells (Mita et al., 2008).

2.4 Glycoprotein

G protein is essential for RV spread. RV SAD-B19 strain was constructed with entire deficiency of the G gene. SADΔG was able to bud itself out of the infected cells but with the retarded rate as compared to wild-type. These viruses were spikeless and not infectious. Nonlethal infection after IC inoculation in adult mice with this G-deleted virus may result from restriction of viral spread in the brain (Etessami et al., 2000).

Some fixed RV strains, possessing arginine or lysine at position 333 of G protein, cause lethal infection in adult mice following IC inoculation. RC-HL strain does not fall into this category; it has arginine at this position. The pathogenicity of this strain may be determined by other, yet unknown, mechanism. Replacing an open reading frame (ORF) of G gene of Nishigahara strain in the backbone of RC-HL strain resulted to significantly

increase in pathogenicity of the chimeric virus (Ito et al., 2001).

Reversion of nonpathogenic RV containing glutamic acid at position 333 of G to pathogenic phenotype could be achieved by a single amino acid substitution. Replacement of asparagine with lysine at position 194 of G resulted to an increase in pathogenicity of this mutant. It also exhibited faster internalization of virus, increased rate of spreading as well as slightly increased in pH threshold during membrane fusion (Mebatsion et al., 2001).

Exchanging G of Nishigahara with Ni-CE strain to become chimeric Ni-CE, however, did not revert the mortality rate of IC-inoculated mice to 100%. Only 20% death rate was observed. Chimeric Ni-CE viruses, containing either Nishigahara N, P or M gene, successfully caused lethal infection in adult mice (Shimizu et al., 2007).

Over the years, it has been convinced that the expression level of RV G is inversely correlated with the virulence. Recent study using codon-optimization method, adopting the idea from "attenuation by a thousand cuts", showed that the amount of G expression might not be the only determinant role in viral virulence as well as in inducing apoptosis. CVS-N2c is a chimeric virus with neither codon-optimized nor condon-deoptimized G. It can express G at fullest or lowest level without altering the structure. It exhibits higher or lower G level than wild-type recombinant virus. However, the most pathogenic virus was the wild-type one with normal expression level of G (Wirblich et al., 2011).

The sequence of G gene also plays role in pathogenicity. Recently, mutation of PDZ-BS domain (PDZ binding site) located at the cytoplasmic domain of G of Evelyn-Rokitnicki-Abelseth (ERA) strain, ETRL, has been reported to play a role in attenuation of rabies virulence by competitive binding to non-receptor protein tyrosine phosphatase 4 (PTPN4), which has anti-apoptotic function. This results in death of infected NA cells through apoptosis mechanism which in turn affects the pathogenicity of the virus. On the other hand, PDZ-BS domain of CVS, QTRL, can inhibit the anti-survival function of microtubule associated serine-threoninekinase 2 (MAST2) resulting in intact neurite growth of infected neurons (Prehaud et al., 2010).

Computational analysis of 53 full-length Lyssavirus G gene sequences from various hosts, ranging from street virus isolates to vaccine strains, over the past 70 years showed that the adaptation of Lyssavirus in the process of spill over, host shift or the development of vaccine strain is not dependent on the evolution of G gene (Tang and Wu, 2011).

 2.2.5 Large protein

L protein functions as enzymatic component of RdRp with replicase and polymerase activities. It recognizes only the RNP form of viral RNA instead of naked RNA as a template. Apart from polymerase activity of L protein, RdRp also plays role in cap methylation of newly synthesized mRNA. The structure and domains of L gene were

described based on the study of vesicular stomatitis virus (VSV), prototype of vesiculovirus. It consists of 6 domains, I to VI, like other negative stranded RNA viruses. The first 4 domains, I to IV, possess enzymatic activities. Domain III contains putative polymerase active site, conserved GDN sequence of motif C. Domain V and VI involve in adding GDP to 5'-end of monophosphorelated mRNA and cap methylation, respectively.

Recombinant VSV containing mutation located at domain VI, D1671V (previously observed in VSV mutant), has abrogation of mRNA cap methylation mediated by methyltransferase activity at both guanine-N7 and 2'-O-adnosine, without disturbing mRNA capping (Grdzelishvili et al., 2005). Another mutation, G1481R (located between domain V and VI), was involved in mRNA cap methylation. Drastic decrease in mRNA cap methylation of recombinant virus with this mutation was observed (Grdzelishvili et al., 2006).

Mutation of domain II, which has been believed to serve as template recognition with highly charged putative RNA binding motif, has impact on RNA synthesis of Sendai virus, a member of paramyxovirus family. Conversion of some charged residues located at the central highly charged conserved region to alanine, uncharged residue, resulted to defect in viral RNA synthesis (Smallwood et al., 1999).

In the case of RV, site-directed mutagenesis was acquired to alter a single amino acid of GDN sequence. These GDN-mutated mutants failed to direct the RNA synthesis due to the lack of polymerase activity (Schnell et al., 1995).

However, chimeric RV containing L gene of pathogenic SHBRV-18 strain in the backbone of non-neuroinvasive RV strain could induce lethal infection in IC-inoculated adult mice at comparable level as recombinant SHBRV-18 virus. Slight decrease in mortality rate of 20% which was lower than SHBRV-18, was observed in mice IM inoculated with this mutant (Faber et al., 2004).

The stability of live attenuated oral vaccine strain, SAD-B19, was performed by serial IC passages into either mice for 10 times or foxes 4 times. The sequences of the passages were determined. No nucleotide substitution was found in mice passages whereas mutations were found in the 4th passage in foxes. There were 7 nucleotide substitutions located in L gene comparing to SAD-B19 sequences, which resulted to one amino acid substitution at position 9240. However, this mutation did not affect the virulence *in vivo* (Beckert et al., 2009).

2.2.6 Non-coding region

Non-coding regions (NCRs) located between each IGR are flanked by transcription termination and transcription initiation signals. In VSV, IGRs are conserved as dinucleotide 3'-GA-5'. However, in the case of RV, which belongs to the same *Rhabdoviridae* family, IGRs located between N/P, P/M, M/G and G/L are 2, 5, 5 and 24-29 nucleotides, respectively. Once RNA polymerase reaches termination signals on mRNA, seven uridine sequences, it starts making polyadenylated tail. Once polymerase complex dissociates from its template, it restarts transcription of downstream target. This

causes the transcription gradient, which results to the decrease in downstream mRNA

expression level, approximately 30% (figure 3) (Wunner, 2007 and Albertini et al., 2011).
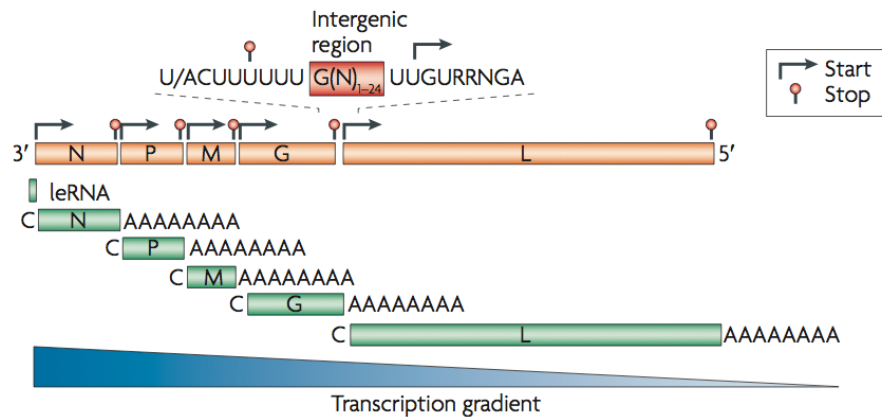
Figure 3 Transcription gradient (Schnell et al., 2010)

Mutations occurred in this region have been proven to play role in viral

transcription/replication.

Nearly all mutations introduced to the first 3 nucleotides of VSV transcription start

sequences had an impact on the reduction of downstream gene transcription level.

Plasmids containing M and G genes of VSV flanked by Le and Tr sequences were

produced. Further mutational analysis of the conserved transcription start sequences

and intergenic dinucleotides was performed. Mutation at the first nucleotide resulted in

the drastic reduction of G downstream transcript expression level. This expression level

was similar with plasmids containing mutation at the second and third nucleotide,

except the second U to C mutant. Most of mutant plasmids with mutation at intergenic

dinucleotides, nucleotide 4, 5 or 8-10 had little effect on G level. However, replacing A of

intergenic dinucleotide (GA) with U resulted in drastic reduction of G expression, possibly due to the shift of transcription start sequence. Pyrimidine may be required at the first nucleotide of transcription start sequence for transcription initiation by polymerase (Stillman et al., 1997).

3'-AUACU$_7$-5' has been proven to be necessary for transcription termination of an upstream transcripts in VSV. Two different minireplicons were generated, the first plasmid containing coding sequences of N and P and the second one only N coding sequence. Both were flanked by Le and Tr sequences. Following transfection of mutant plasmids, read-through N-P transcripts were observed in U$_7$-deleted, AUAC-deleted and GA intergenic dinucleotides mutants. The former gave rise to the highest level of read-through transcript with failure to terminate upstream and reinitiate downstream transcripts. Failure to reinitiate downstream transcript, UUGUC-deleted mutant had no effect on terminating upstream transcript. Mutation at U$_7$ stretch also affected the polyadenylation. Shortening of uridine stretch and disruption between AUACU$_7$ enhanced the amount of read-through transcripts. Thus, AUACU$_7$, not U$_7$ stretch alone, was required for termination of the transcript (Hwang et al., 1998).

Barr JN in 1997 documented the role of conserved AUACU$_7$ on transcription termination of VSV. Plasmids containing partial N, P and L coding sequences, flanked by Le and Tr sequences were generated. Impaired termination of mRNA transcript was the consequence of mutation at AUAC sequence. Total abrogation of termination was

observed in mutation at the last C. Moreover, AUAC sequence alone was not sufficient to facilitate the mRNA termination. The minimum number of uridine stretch required for terminating upstream transcript was 7. Shortening of this U7 tract, U0, U5 and U6, entirely abolished this ability. Doubling the size of U7 to U14 did not increase termination efficiency; in contrast, U14 mutant severely impaired the reinitiation of downstream mRNA. Further, mRNA termination was also affected by replacing U7 with A7. Mutation at the third or seventh U tract resulted in the complete abrogation of termination ability (Barr et al., 1997).

Length of IGR has been shown to be critical for gene expression level. Minigenome containing N/P IGR flanked by chloramphenicol acetyltransferase (CAT) and firefly luciferase gene was generated. The function of RV IGR on gene expression level was determined by replacing the N/P IGR with P/M, M/G or G/L. Slightly increased read-through transcripts were observed, thus, the transcription termination was not likely to be affected by different IGRs. Nonetheless, the expression level of downstream transcripts was enhanced. This was in accordance with the results obtaining from full-length cDNA clones. Both mutant recombinant viruses, SAD T, acquiring N/P IGR instead of G/Land SAD T2, with M/G and G/L IGR replacement exhibited higher L mRNA and protein expression comparing to wild-type virus. However, CPE was strongly induced in both mutant viruses, with the former to the lesser extent. Paralysis of the mice was observed following peripheral inoculation of SAD T2 viruses (Finke et al., 2000).

The orientation of the genes also has an impact on the expression levels due to transcription gradient. Construction of full-length cDNA plasmid of ERA strain with switching between G and M gene resulted to ERAgm recombinant viruses, with N-P-G-M-L gene order. Comparing to its parental strain with similar viral growth, ERAgm recombinant virus exhibited enhanced G gene expression in BSR infected cells due to the transcription gradient as described above. The pathogenicity in mice was attenuated as a result of higher G expression (Wu et al., 2008).

2.7 Passage of rabies virus in heterogeneous host

Passaging of RV has been done in order to amplify and maintain viruses, with the generation of fixed or vaccine strains.

RV SAD strain was passaged several times in BHK cells resulting in SAD-B19 strain, which was widely used as oral vaccine for foxes in Europe (Vos et al, 1999).

Passaging of CVS-24; challenge virus standard,that has been maintained in suckling mice, into two different hosts resulted to different phenotypes. CVS-N2c was derived from passaging CVS-24 twice in mouse NA cells whereas CVS-B2c was derived from passaging CVS-24 twice in non-neuronal, BHK-21, cells. The former variant had the ability to cause lethal infection in both neonatal and adult mice by IC route. Attenuation in the ability to kill adult mice was demonstrated in CVS-B2c (Morimoto et al, 1998).

RC-HL strain was used as animal vaccine in Japan. It was generated by passaging of Nishigahara strain into chicken embryos 294 times, 8 passages in chicken embryo fibroblast (CEF), 5 passages in Vero cells and 23 passages in hamster lung (HmLu) cells (Ito et al., 2001).

Nishigahara strain has also been used to generate another attenuated strain, Ni-CE. It was derived from passaging Nishigahara strain 100 times in chicken embryo fibroblast cells. High degree of attenuation was observed in the former, causing non-lethal infection in adult mice and CPE of infected NA cells. Nishigahara strain was able to kill adult mice following IC and did not cause CPE in NA cells (Mita et al., 2008).

CHAPTER III

MATERIALS AND METHODS

Viruses and cells

The RV QS-05 strain was directly isolated from the brain of a Thai rabid dog. It was amplified once in suckling mice brain (SMB) to obtain 20% brain suspension of stock seed virus. This isolate was then serially passaged 7 times in BHK-21 cells, designated as QS-BHK-P7.

BHK-21 and NA cells were maintained in Minimum Essential Medium Eagle (MEM) with 10% fetal bovine serum.

Rabies Virus Titration in NA cells

NA cells were infected with QS-05 or QS-BHK-P7 viruses. Two days post infection, cells were fixed with 90% freshly prepared acetone. Cells were stained with FITC-conjugated antibody to rabies for N (Fujirebio Diagnostics Inc, USA) examined under a fluorescent microscope (see appendix A).

Calculation of median tissue culture infectious dose (TCID50)

TCID50 represents the dose that gives rise to 50% of infected field of inoculated cultures.

1. Calculate difference of logarithms

$$= \frac{50\% - (\text{infectivity next below } 50\%)}{(\text{infectivity next above } 50\%) - (\text{infectivity next below } 50\%)} \times \text{logarithm of dilution factor}$$

2. Calculate log (reciprocal of 50% end-point dilution)

= log (reciprocal of starting point dilution) – difference of logarithms

3. Therefore, $\text{TCID50} = 10^{-\text{calculated value obtained from 2.}}$

Mouse inoculation test

QS-05 and QS-BHK-P7 were diluted in chilled 2%DMEM to obtain 2, 10,100 and 500 TCID50 and kept on ice during the test. A group of five 6-week-old female mice were inoculated with either 30ul of RV intracerebrally (IC) or 50ul of RV intramuscularly (IM). The weight of each mouse was recorded on a daily basis. The clinical disease signs and symptoms were observed and scored daily for 21 days. Any death occurring after the first 5 days was recorded and discarded. The criteria for scoring was 1 = weight loss, 2 = ruffled fur, 3 = paralysis and 4 = moribund and death.

Primer design

Primers were designed based on RV strain 8743THA (accession number EU293121) (Table 1).

Table 1 Primers used in the whole genome amplification

Fragment	Primers Name	Sequences (5'-3')	Position as on QS-05
1	CN1	CTACAATGGATGCCGAC	66-82 (F)
	CN4	GGATTGAC(AG)AAGATCTTGCTCAT	1514-1536 (R)
2	RabPfor	TTACTTCTCCGGTGA(GA)AC(GA)AGGAG	1247-1272 (F)
	RabPrev	GAGG(GA)TTTTTGAGTGTCCTC(GA)TC	2532-2554 (R)
3	RabM (F)	TGATCTGAACCGTTATACATCCC	2381-2403 (F)
	RabM (R)	AAACAAAAGAGCCTGAGGAATC	3318-3339 (R)
4	RabG1.2a	TCTGGTGTATCAACATGAAC	2998-3016 (F)
	RabG1.2b	GACTTGGTGGTCATGATAGAC	4236-4256 (R)
5	RabG1.5a	AGACCTGTGGATTTGTGGACGA	3986-4007 (F)
	RabG1.5b	GTTCAGCCTCTAACTCGATT	5451-5470 (R)
6	RabL1 F	CTGTGGAACAGAAGGACAAT	5356-5375 (F)
	RabL1 R	CCTGAACTTCTCTGCCCTCT	6341-6360 (R)
7	RabL2 F	CTCCGGTTATGAAGTCATTAAAAT	6285-6309 (F)
	RabL2 R	ACATCTTCTGTTGACTCCAACC	7289-7310 (R)
8	RabL3 F	GGTTACATATGCCTTTCACCTG	7239-7260 (F)
	RabL3 R	CTCTCCAAG ATTGGATTCC	8243-8262 (R)
9	RabL4 F	ATCTGGCTGAGCTCCCATGA	8191-8210 (F)
	RabL4 R	CTGTACTTACGGAGATATGAGAGAG	9190-9214 (R)
10	RabL5 F	CAAGTCTGCTAGATACAGTGA AGG	9138-9161 (F)
	RabL5 R	AGATTCTAAGGTGTCCTCTCCATG	10147-10160 (R)
11	RabL6 F	GCATGAGAACTAACCTGCGA	10091-10110 (F)
	RabL6 R	GCCCTCTGCATCTCACTCTT	11119-11138 (R)
12	RabL7 F	GCTGTACCTCAGATTCTCCAAG	11010-11031 (F)
	RabL7 R	CAGCTAGAGGTTCTGACTTGAG	11861-11882 (R)
3'RACE	CN10	AGGAGTGATCTTGTCTCCTTT	385-365 (R)
	RabN 334R	CGACAAGATTCCATAACTGGTCCAG	334-355 (R)
5'RACE	RabL 11389F	CCGTCTGACCCCAAGATCTTGA	11389-11410 (F)
	RabL 11411F	GGCACTTCAATATCTGCTGCAGT	11411-11433 (F)
	RabL11463F	TGATGTCCCCAGCTTTGCAAG	11463-11483 (F)

RNA isolation

Total RNA was extracted from brain suspension, QS-05, or cell supernatant, QS-BHK-P7, using High Pure Viral RNA Kit (Roche, Germany) according to manufacturer's protocol.

Reverse Transcription

cDNA was synthesized by mixing 1ug of total RNA, 1ul of random primer (Promega) and nuclease-free water to a final volume of5ul in 200ul-thin-wall tube. The mixture was heated at 70°C for 5 min, then immediately chilled on ice or 4°C for 5 min. The reaction was transferred to ImProm-II^{TM} Reverse Transcription reaction tube containing 4ul of ImPromII 5x reaction buffer, 2.4ul of 25mM MgCl$_2$, 1ul of 10mM dNTP, 0.5ul of RNase Inhibitor, 1ul of ImPromII Reverse Transcriptase and nuclease-free water to a final volume of 15ul and incubated at 25°C for 5 min followed by 42°C for 1 hour and 70°C for 15 min. cDNA was immediately used as a template for polymerase chain reaction or stored at -20°C.

Polymerase Chain Reaction Amplification (PCR)

Polymerase chain reaction was performed using Phusion$^{®}$ High-Fidelity DNA polymerase (Finnzymes, Finland) on GeneAmp$^{®}$ PCR System 9700 (Applied Biosystems, USA). Briefly, 5ul of cDNA was amplified with 5x Phusion$^{®}$HF buffer, 10pmol of each primer (forward and reverse), 10mMdNTP and 0.5 U of Phusion$^{®}$ DNA polymerase. The

cycling profile was as followed; 98°C for 30 seconds, initial denaturation, followed by 30

cycles at 98°C for 10 seconds, 55°C for 30s and 72°C for 30 seconds/kb, and final

extension at 72 ^{o}C for 10 min. PCR products were confirmed by agarose gel

electrophoresis and visualized by ethidium bromide staining (under UV illumination) with

1 kb DNA marker (Fermentas, USA). The gels containing expected PCR products were

excised and DNA was purified using QIAquick Gel Extraction Kit (QIAGEN, USA)

according to manufacturer's protocol.

3' and 5' untranslated region (UTR) amplification

3' and 5' end of rabies genome were amplified using 3' RACE System for Rapid

Amplification of cDNA Ends and 5' RACE System for Rapid Amplification of cDNA Ends,

version 2.0 (Invitrogen, USA), respectively.

3' RACE

1. First strand cDNA synthesis, 1ug of total RNA was used along with oligo(dT)-
   containing adapter primer, SuperScript^{TM}II RT and reaction buffer.

2. 2ul of cDNA was then added to PCR reaction containing Abridged Universal
   Amplification Primer (AUAP) and CN10 reverse primer.

3. Heminested PCR was performed using PCR product and AUAP and RabN334R
   (reverse primer), cycling profile as described above.

<u>5' RACE</u>

1. First strand cDNA was synthesized from total RNA using RabL11389 forward primer, gene-specific primer (GSP1), and SuperScript™II RT.

2. Removal of mRNA template by adding 1ul of RNase Mix and incubated at 37°C for 30 minutes

3. Separation of cDNA from unincorporated dNTPs, GSP1 and proteins by S.N.A.P Column.

4. Homopolymeric tail was added to the 3'-end of cDNA using TdT and dCTP following

5. The dC-tailed cDNA was amplified using AUAP and RabL11411 forward primer.

6. Heminested PCR was performed using PCR product and AUAP and RabL11463 forward primer, cycling profile as described above.

Indirect sequencing

The G1.2 and G1.5 PCR fragments were amplified from 1 ug of cDNA with primers RabG1.2a and RabG1.2b, and RabG1.5a and RabG1.5b, respectively. The second round PCR was performed using the combination of G1.2 and G1.5 PCR products as template with RabG1.2a and RabG1.5b primers. PCR products were cloned into pGEM-T $^{®}$ easy vector system (Promega). Twenty white colonies were picked up and the purification of plasmids was performed using Nucleospin$^{®}$ Plasmid (Macherey-Nagel, USA). The purified plasmids were sequenced (see appendix B).

Sequencing

Purified DNAs or plasmids were commercially sequenced (1st Base, Malaysia).

Sequence alignment and Analysis

The sequences were analyzed using 4Peak. Multiple sequence alignment and identity of nucleotide and amino acid was performed using MEGA5.

CHAPTER IV

RESULTS

1. Passages of canine street rabies virus (QS-05) in non-neuronal cells yielded phenotypic differences

TCID50 of both RV was determined by virus titration in *in vitro*. NA cells were infected with 10-fold serial dilution of either QS-05 or QS-BHK-P7. Forty-eight hours post infection (pi), immunofluorescent (IF) staining of RV N was performed. Thirty fields per each dilution were counted. At least one infected cell was counted as positive field. TCID50 of QS-05 and QS-BHK-P7 were $10^{-2.7}$ and $10^{-3.1}$ respectively. In order to characterize the *in vitro* phenotype of both viruses, NA cells were infected by QS-05 and QS-BHK-P7 at the concentration of 50 TCID5. IF staining of RV N was performed 1 to 4 day(s) pi.

On day 1 pi, there were less than 10% of cells infected in the case of QS-05. This was seen as tiny dot-like IF particles. The IF pattern was unchanged on day 2 pi, however, slight increase in numbers of infected cells was observed. Approximately 30% of cells were infected on day 3 which was increased to 60% on day 4 pi. Foci formation, representing spreading of virus to neighboring cells, was noted by day 3 pi with no change on day 4 pi. In the case of QS-BHK-P7, large IF particles were observed since day 1 pi, and became remarkably larger and more vivid until day 4 pi. Approximately

10% of cells were infected on day 1 which was increased to 60% and 100% on days 3

and 4 pi respectively. Abundant foci formation was seen on day 3 (first detected on day

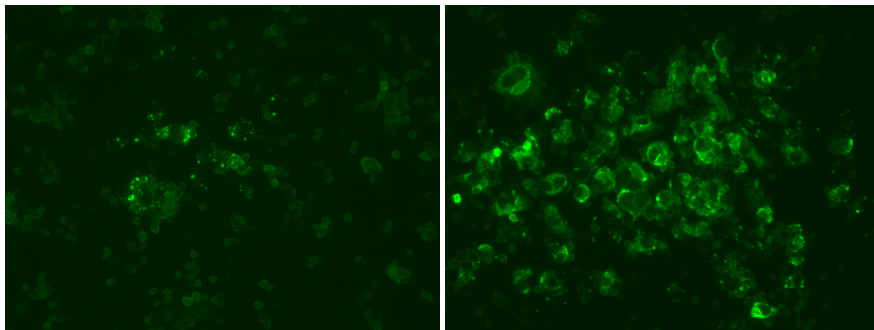2) and was profound on day 4 pi (figure 4).
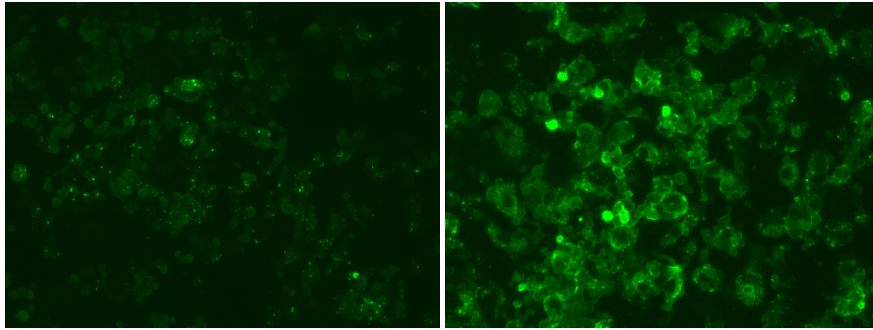
(a)
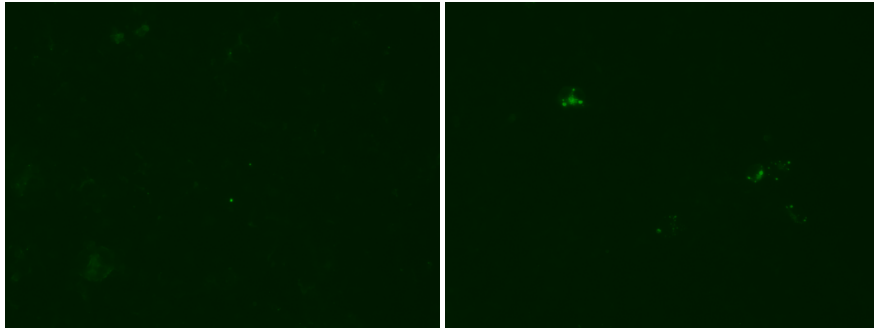
(b)
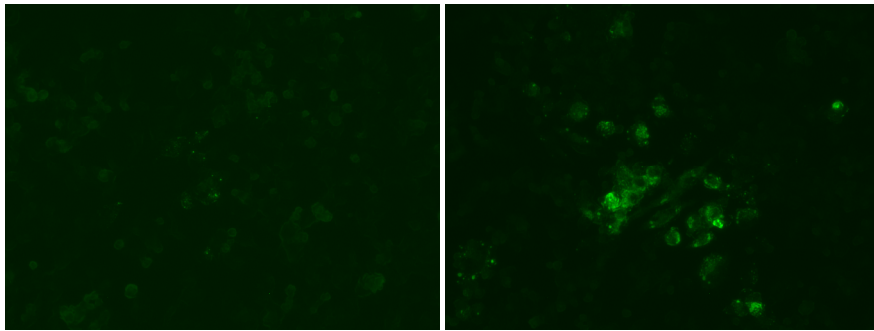
(c)

(d)

Figure 4 IF staining of infected NA cells. NA cells were infected with QS-05 (left) or QS-

BHK-P7 (right). IF staining of infected cells was performed on 1 (a), 2 (b), 3 (c) and 4 (d)

day(s) pi. Green fluorescent staining represented RV N.

## 2. Increase neurovirulence was observed in non-neuronal passage (QS-BHK-P7)

To determine whether *in vitro* result would correlate with *in vivo* system, pathogenicity study of both viruses was performed. A group of 5 six-week-old female ICR mice (average weight of 20 grams) were inoculated 0.03 ml IC or 0.1 ml IM with QS-05 and QS-BHK-P7 at 500, 100, 10 and 2 TCID50. The weight of each mouse was recorded on a daily basis. The clinical disease signs and symptoms were observed and scored daily for 21 days. Any death occurring during the first 5 days was recorded and discarded. The criteria for scoring was 1 = weight loss, 2 = ruffled fur, 3 = paralysis and 4 = moribund and death. IC inoculation of parental QS-05 caused 100% mortality rate at a concentration 500, 100 and 10 TCID50. One mouse survived after 21 days pi at a concentration of 2 TCID50, resulted to 83% mortality rate. In contrast, mortality rate was 100%   in mice IC inoculated with all doses of QS-BHK-P7 (figure 5). None of mice IM inoculated with QS-05 died even with the dosage of 500 TCID50. Mortality rate of mice IM inoculated with QS-BHK-P7 at 500 and 100 TCID50 was 80% and 40%, respectively (figure 6). The initial clinical onset of these IM-infected mice was between 9 to 13 day pi with disease progression to death between 2 to 4 days after the onset. RV was confirmed in all dead mice.

The onset of disease (body weight loss) in mice IC inoculated with both viruses was usually between 5 and 6 days in all groups. QS-BHK-P7 inoculated mice died faster than QS-05 by IC inoculation at all doses after onset. The longest survival period of QS-

05 inoculated mice was 8 days (5 days in QS-BHK-P7) (figure 7). There was an exception in a group of mice IC inoculated with 10 TCID50 of QS-BHK-P7. One day delay of onset at day 7 pi was noted. However, greater degree of weight loss was observed (range between 3-7 grams versus 2-4 grams in other groups at onset), subsequently followed by rapid death.

(a)

QS-05

(b)
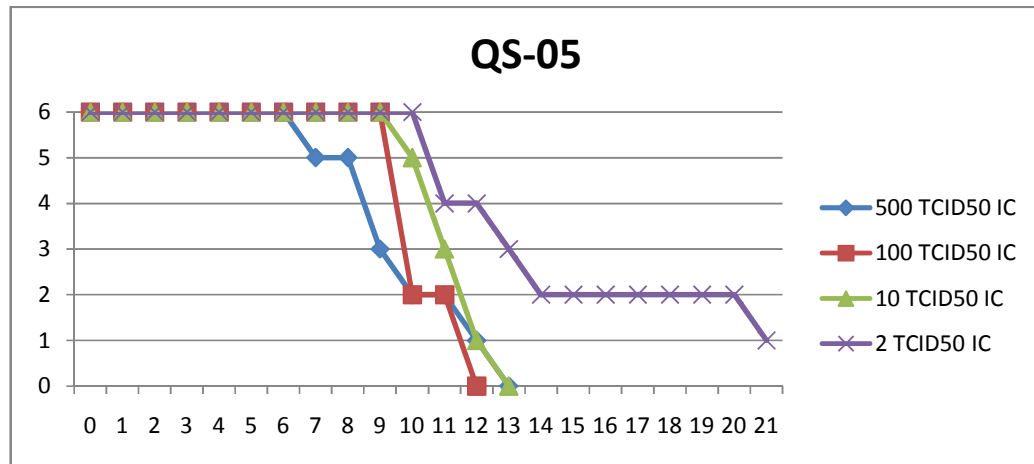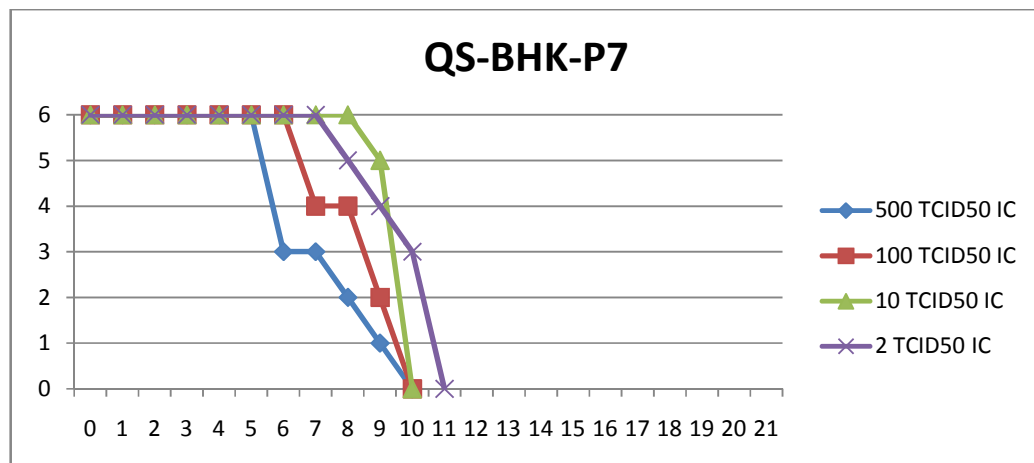
QS-BHK-P7

(c)
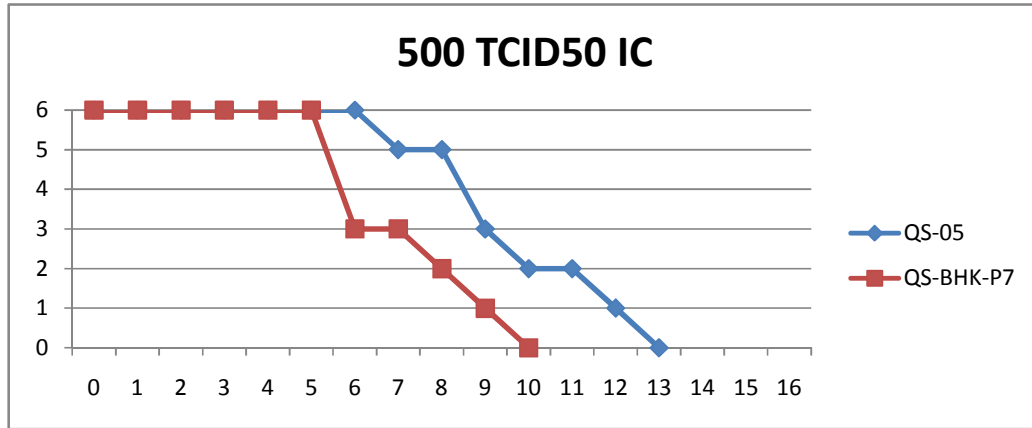
(d)
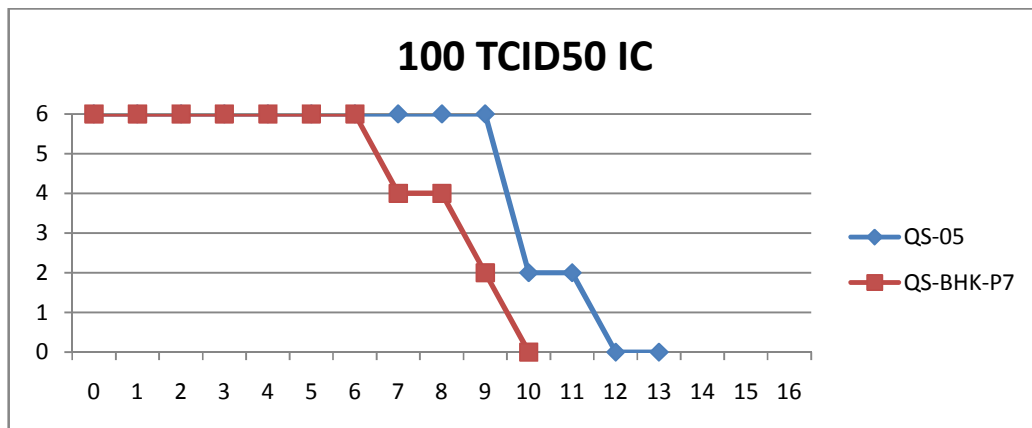
(e)
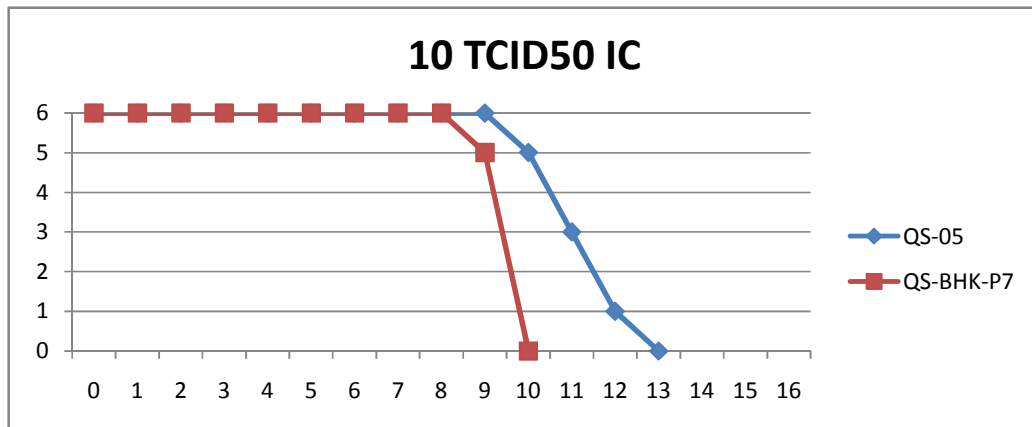
(f)
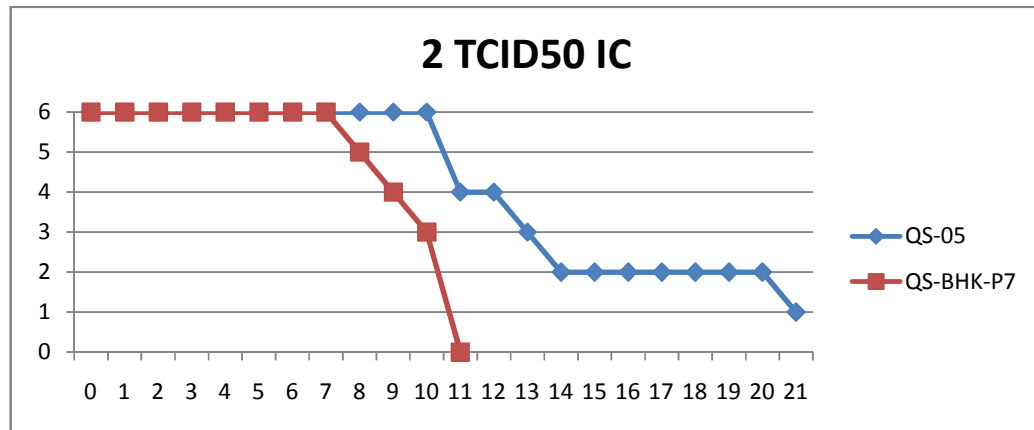
Figure 5 Survival rate of mice IC inoculated with QS-05 (a) and QS-BHK-P7 (b) at concentration 500 (c), 100 (d), 10 (e) and 2 (f) TCID50: Y-axis indicated the numbers of survived mice; x-axis indicated days post inoculation
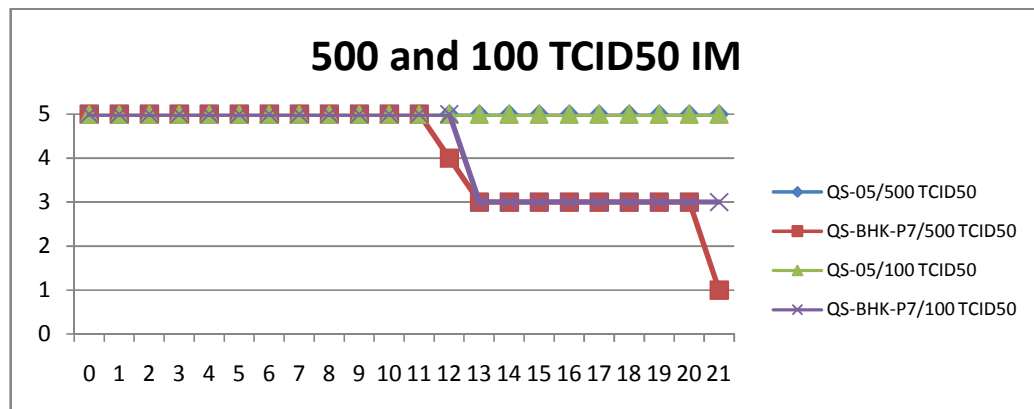
Figure 6 Survival rate of mice IM inoculated with QS-05 and QS-BHK-P7 at concentration 500 and 100 TCID50: y-axis indicated the numbers of survived mice; x-axis indicated days post inoculation

(a)
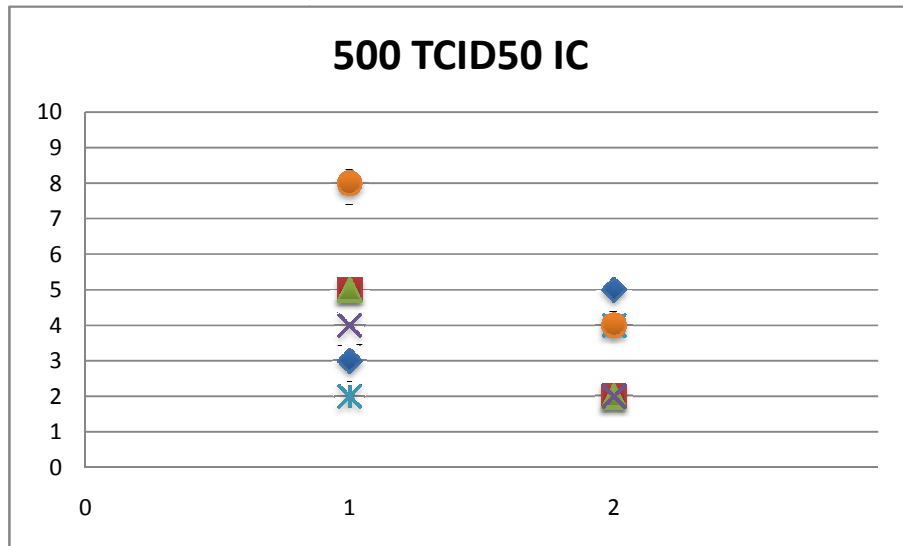
(b)
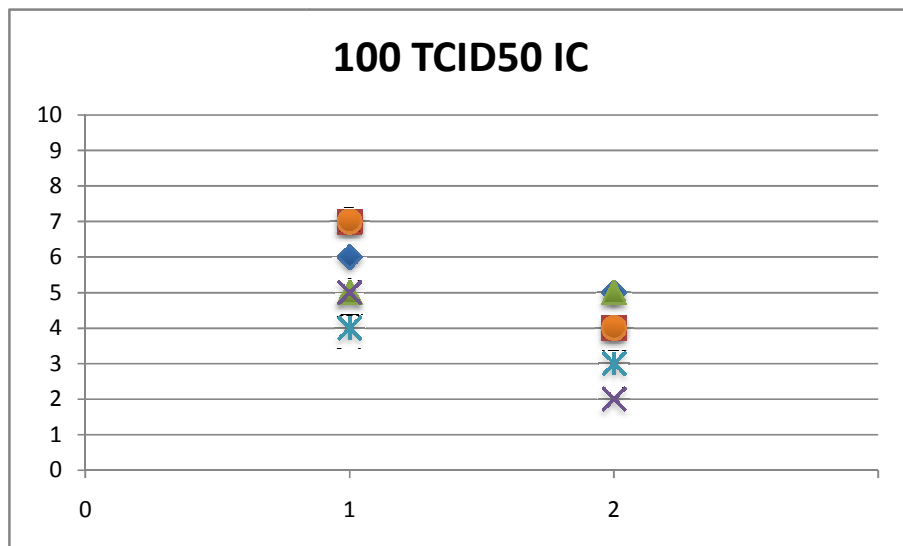
(c)
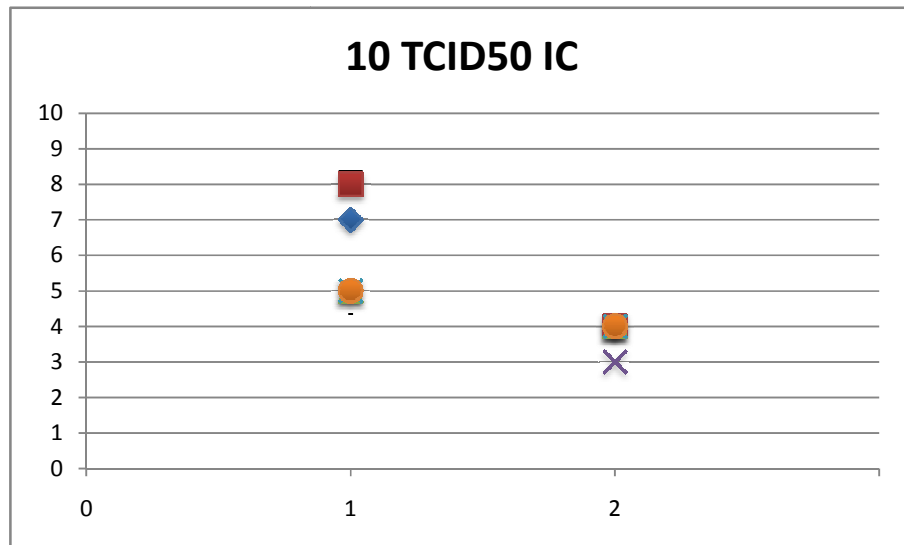
(d)
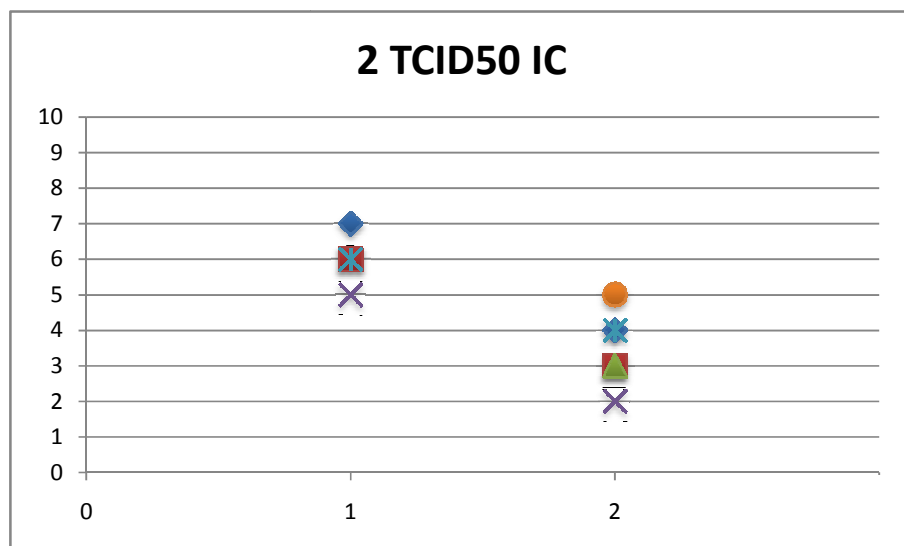
Figure 7 Disease progression after the initial clinical onset in IC inoculated mice with QS-05 (1) and QS-BHK-P7 (2) at each concentration: y-axis indicated the number of days since clinical onset to death

3. Sequence organization of whole genome

Whole genome sequencing was performed to determine whether there were differences that might explain why QS-BHK-P7 became more virulent with an ability to cause disease by both IC and IM routes. QS-05 and Qs-BHK-P7 were 11,923 base pairs consisting of five coding regions, N (71-1423), P (1515-2408), M (2496-3104), G (3316-4896), and L (5407-11793). The first 58 base pairs were 3' untranslated region (UTR), known as Le, and the last 70 base pairs were 5'UTR, known as Tr sequences. IGRs located at each gene junction were 2, 5, 5, 24 base pairs, respectively.

Comparison of whole genome sequences (WGS) of both viruses was performed. No mutation was found between the parental strain, QS-05, and its non-neuronal, QS-BHK-P7, in N, P and M genes, consistent with the fact that these three genes are fairly conserved in RV. Le and Tr sequence were also identical in both viruses. There were 4 mutations found in QS-BHK-P7 as compared to its parental QS-05 virus (figure 8).

Two missense mutations were placed in G gene. The first 19 amino acids of G gene are signal sequences. Therefore, the first amino acid is actually located at the 20th position on G protein. These missense mutations, 3441T>G and 4643A>C, were both located in the ectodomain of G in QS-BHK-P7. These caused 2 amino acid substitutions, S23R (serine to arginine) and H424P (histidine to proline), respectively.

Another missense mutation was found in L gene of QS-BHK-P7. This mutation, 10537A>G resulted to amino acid substitution I1711V (isoleucine to valine). All sequences located across every gene junctions of QS-05 and QS-BHK-P7 were identical except for P-M gene junction. One point mutation, 2475A>G, located at non-coding region between P and M genes of QS-BHK-P7 was demonstrated. This mutation lay at the 7th adenine residue of poly (A) sequence.

Comparison between QS-BHK-P7 and its parental QS-05 revealed 99% identity at nucleotide and amino acid levels. The identity of nucleotides between these two viruses and 8743THA, Thai street strain, was 98%.

The GenBank accession numbers of QS-05 and QS-BHK-P7 were JN786877 and JN786878, respectively.

(a)
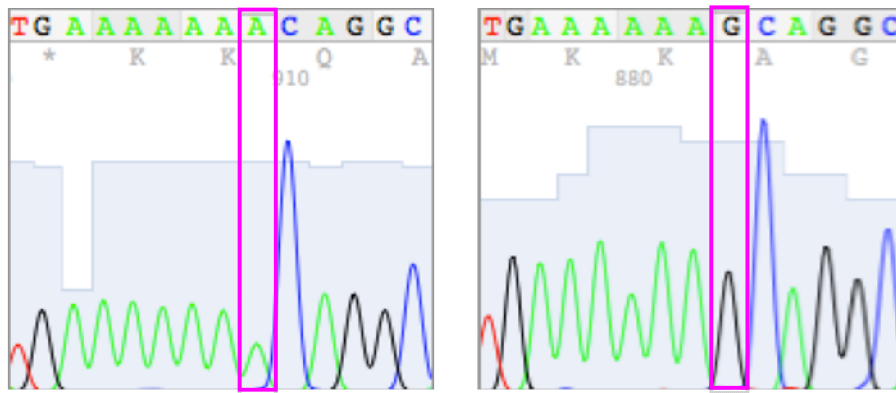
(b)
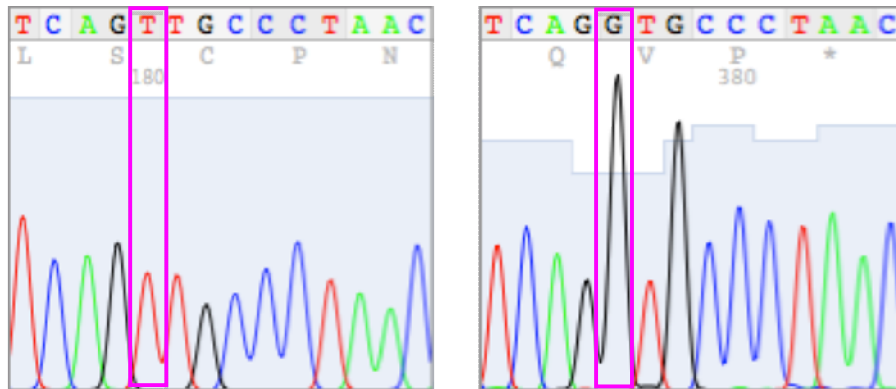
(c)
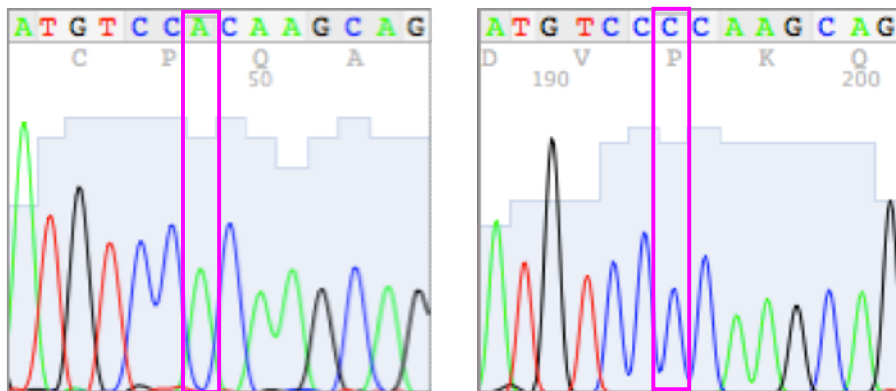
(d)
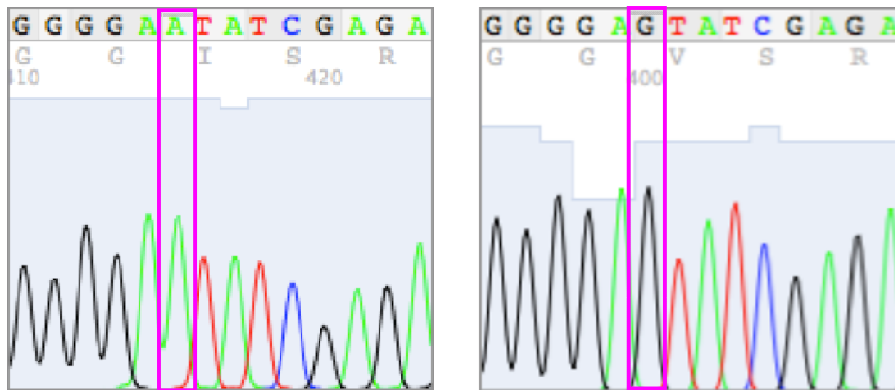
Figure 8 Nucleotide substitutions of QS-BHK-P7 (right) in comparison to QS-05 (left), 2475A>G (a), 3441T>G (b), 4643A>C (c) and 10537A>G (d): the number indicated the nucleotide position on WGS.

4. Genetic diversity of glycoprotein gene

To determine whether the amino acid substitutions at positions 23 and 424 of G of QS-BHK-P7 were the result of adaptation to the new environment, indirect sequencing of QS-05 and QS-BHK-P7 clones of G gene was performed. In QS-05, all 20 clones had identical nucleotide sequences compared to its direct sequencing. All 20 clones of QS-BHK-P7 had S23R amino acid substitution, which located at the ectodomain of RV G. Thus, the substitution at this position might represent the adaptation in non-neuronal cells. This should also be the same as in the case of position 424. H424P amino acid substitution was found in 19 of 20 clones of QS-BHK-P7. The other clone had proline as found in QS-05.

CHAPTER V

DISCUSSION AND CONCLUSION

We demonstrated that adaptation of dog virus variant in non-neuronal cell line, after 7th passage in BHK-21 cells, resulted in altered morphologic appearance of viral particles as examined by fluorescent antibody staining of infected NA cells. At 50TCID50 dose, the number of NA cells infected with QS-BHK-P7 was increased more rapidly than QS-05 infected one as visualized by IF. Viral spread to adjacent cells of the former was also faster. Foci formation could be observed as early as day 2 pi, while QS-05 on day 3 pi but with lesser extent. Both viruses also had difference in IF patterns of infected cells. QS-05 had tiny dot-like pattern, whereas viral particles of QS-BHK-P7 in cytoplasm of infected cells appeared remarkable larger in size. Further, QS-BHK-P7 was able to cause mortality in adult mice by both IC and IM challenges whereas parental isolate, QS-05 could only kill by IC route. In addition, mice IC-inoculated with QS-05 had prolonged clinical course after clinical onset as compared to that observed in QS-BHK-P7 inoculated mice.

Such findings were intriguing since RV pathogenicity usually became attenuated following passages in non-neuronal cells. These included SAD-B19, oral vaccine strain, passages of SAD strain in BHK cells (Vos et al., 1999), CVS-B2c (CVS-24 in non-neuronal cells, BHK-21 cells) (Morimoto et al., 1998). The latter contained a S23R mutation in G gene; with higher replication rate than in the parental strain. CVS-B2c was

less neurotropic, both in vitro and in vivo, compared to CVS-N2c. Nishigahara strain was derived from the original Pasteur strain before 1915 and had divergence at non-coding pseudogene region (Sakamoto et al., 1994). It was serially passaged through several kinds of animals and cell cultures and was used as seed strain for animal vaccine production. Non-pathogenic Ni-CE came from the Nishigahara strain after passages in CEF cells (Mita et al., 2008).

Alteration of viral transcription/replication, budding and immune evasive mechanism and spreading can affect the pathogenicity of virus (Cenna et al., 2009, Finke et al., 2000 and 2003, Masatani et al., 2010 and 2011 and Shoji et al., 2004). This has been demonstrated by modification of rabies viral gene(s) by reverse genetics technique (Albertini et al., 2011, Okumura et al., 2011 and Lafon, 2011). Higher replication rates and degree of apoptosis are inversely correlated with pathogenicity. Pathogenicity also depends on how well virus can evade the immune system (Finke et al., 2003, Prehaud et al., 2010, Pulmanausahakul et al., 2008 and Wang et al., 2005). Enhancement of neuroinvasiveness following IM inoculation has been observed after replacement of G or G and M genes of SAD-B19 by silver-haired bat-associated RV strain 18 (SHBRV-18) (Pulmanausahakul et al., 2008).

Homeostasis in RV replication/transcription is balanced by interaction between N, P and L genes. Failure to phosphorylate N resulted in the reduction of replication and transcription (Wu et al., 2002). Over-expression of L gene resulted in enhanced RNA

replication and in higher virus titer. Such imbalanced protein expression also affected the degree of CPE of infected cells expression (Finke et al., 2000). Multifunctional M protein can regulate transcription and replication. Attenuation of M expression, by translocation of M gene to downstream of L gene, yielded a lower replication level (Finke et al., 2003). As previously mentioned, Ni-CE was derived from Nishigahara strain. Clear CPE in mouse NA cells has been demonstrated after infection with Ni-CE but not with parental Nishigahara strain. M protein of the Ni-CE strain had a single amino acid substitution at position 95. This is a cytopathic determinant in mouse NA cells (Mita et al., 2008). Apoptosis also plays a role in this.

Budding of RV occurs at the plasma membrane of the host cells (Okumura et al., 2011). This process requires G and M expression. Although the recombinant SAD-L16 strain (lacking of the entire G gene) could produce a non-infectious spike-less virion, virus release was decreased by 30-fold. M-deleted mutant has been shown to increase G expression at the infected-cell surface with a drastic decrease in infectious virion (Mebatsion et al., 1999).

Evasion of the host immune response is one of the important characteristics of pathogenic RV (Lafon, 2011). This is influenced by both G expression and sequences. An inverse relationship between pathogenicity and the amount of G produced in infected cells has been documented (Wang et al., 2005 and Wu et al., 2008). Compared to the pathogenic SHBRV strain, the attenuated RV strain, laboratory-adapted virus B2c,

expressed higher G level and triggered a greater immune response (Wang et al., 2005).

A reshuffled ERA RV with the G gene switched with the M gene (N-P-G-M-L versus N-P-M-G-L of parental strain) conferred higher G expression according to the transcription gradient mechanism and resulted in less virulent phenotype comparing to parental strain (Wu et al., 2008).

Expression level of the G gene alone is not the sole mechanism in attenuating pathogenicity (Faber et al., 2007 and Wirblich et al., 2011). Sequences within the G gene also play a role in determining the virulence of the virus. Recombinant nonpathogenic live RV vaccine, which has two G genes with R333E, is able to control N194K mutation. Mutation at position 194 is associated with a reversion to the pathogenic phenotype (Faber et al., 2007). Recombinant viruses codon-optimized G and sequences unaltered from highly pathogenic wild-type parental strain, but with 2-3 folds more of the G expression, remained pathogenic (Wirblich et al., 2011).

Recently, ERA strain of RV has been demonstrated to encode a carboxyl-terminal PDZ domain-binding motif within cytoplasmic domain of G gene that interacts with cellular PDZ proteins; serine-threonine kinases, MAST1 and MAST2 (Prehaud et al., 2010 and Javier et al., 2011). These cellular protein targets control neuronal survival that promotes spreading and virulence of RV. Only a single amino acid change in this domain triggered apoptotic death of infected neurons resulting to attenuation of RV. However, the difference in the degree of pathogenicity between QS-05 and QS-BHK-P7

should not be explained by alteration of functional cellular PDZ proteins. Both of them share identical sequences of cytoplasmic G domain.

Computational analysis of lyssavirus G sequences from different hosts showed no positive selection, which represented the adaptation, despite the fact that G is the only protein interacting with the outer environment (Tang K and Wu X, 2011).

Both mutations at ectodomain of G gene should not be responsible for an increased neurovirulence of QS-BHK-P7. Amino acid substitution located at position 23 of G gene has already been shown to be the non-neuronal adaptation marker of the CVS-adapted strain, CVS-B2c, with attenuated pathogenicity (Morimoto et al., 1998). This finding was consistent with the indirect sequencing result of all 20 colonies of QS-BHK-P7 that possessed S23R mutation. Owing to the lack of supporting study, the impact of the other mutation, H424P, on pathogenicity is still unknown.

The mutation in L gene of QS-BHK-P7 is intriguing. D1671V mutation within domain VI and G1481R between domains V and VI of vesicular stomatitis virus (VSV) L protein inhibited viral mRNA cap methylation and further reduced transcription and replication in vitro (Grdzelishvili et al., 2005 and 2006). In the case of Sendai virus, alanine substitution at charged residues in conserved domain III affected viral protein stability and might attenuate pathogenicity (Smallwood et al., 1999). Abrogation of polymerase activity in RV was accomplished by altering the GDN sequence in motif C (Schnell et al., 1995). However, replacement of L gene of pathogenic strain, SHBRV-18,

with vaccine strain, SAD-B19, did not alter pathogenicity of the recombinant virus (Faber et al., 2004). Besides, one amino acid substitution in L gene, which was found following 4th passage of SAD-B19 strain in foxes, did not affect the virulence *in vivo* (Beckert et al., 2009). Thus, the importance of missense mutation in L gene of QS-BHK-P7, which does not reside in 6 documented functional domains, on virulence is still inconclusive.

Non-coding sequences located between coding gene regions or IGR, have been reported to play a role in viral pathogenicity and gene expression (Albertini et al., 2011). Transcription gradient occurs as a result of the dissociation of polymerase complex when it reaches transcription stop signal between each gene junction in rabies (Wunner, 2007). Re-initiation of downstream gene transcription, therefore, is lower than in the predecessor at approximately 30%. The IGR length has impact on rabies gene expression. Overexpression of L gene was achieved by replacing G/L (24 nucleotides) with N/P (2 nucleotides) IGR (Finke et al., 2000). Relocation of M with G gene in ERA recombinant virus resulted in increased G expression and attenuated phenotype (Wu et al., 2008). This emphasizes the importance of the gene order. The sequences per se are involved in viral virulence. In the case of VSV, mutation of the intergenic dinucleotide sequences increased read-through mechanism across the P/M gene junction (Stillman et al., 1997). Deletion of conserved $AUACU_7$ sequences, polyadenylation signal of VSV, resulted in the loss of transcription termination of upstream transcripts (Hwang et al., 1998). Seven U residues was the minimum number required for transcription termination

of upstream mRNA. Shortening or complete deletion of U7 tract or nucleotide substitution at the 7thU of U7 tract gave rise to the read-through transcripts (Barr et al., 1997).

We hypothesize that A>G mutation at the 7thpolyadenylation sequence located between P and M gene junction may result to the read-through transcripts, with the assumption that G of QS-BHK-P7 variant is well adapted to support the spread of the virus. Owing to the transcription gradient and the read-through mechanism of polymerase across P/M IGR, we hypothesize that this may lead to alteration of M expression but may increase G expression in QS-BHK-P7 variant. The former should have an impact on viral budding, transcription/replication and immune evasive strategy that overcome the effect of over-expression of G. The precise mechanism on how these mutations involved in the increased virulence of non-neuronal adapted variant, remains to be further elucidated.

REFERENCES

Albertini A.A., Ruigrok R.W., and Blondel D. Rabies virus transcription and replication. Adv Virus Res.79 (2011):1-22.

Barr, J. N., Whelan, S. P., and Wertz, G. W. cis-Acting signals involved in termination of vesicular stomatitis virus mRNA synthesis include the conserved AUAC and the U7 signal for polyadenylation. J Virol.71(11)(1997):8718-8725.

Beckert A., Geue L., Vos A., Neubert A., Freuling C., and Muller T. Genetic stability (in vivo) of the attenuated oral rabies virus vaccine SAD B19. Microbiol Immunol.53(1)(2009):16-21.

Brzózka K, Finke S, Conzelmann KK. Identification of the rabies virus alpha/beta interferon antagonist: phosphoprotein P interferes with phosphorylation of interferon regulatory factor 3. J Virol.79(12)(2005):7673-7681.

Brzózka K, Finke S, Conzelmann KK. Inhibition of interferon signaling by rabies virus phosphoprotein P: activation-dependent binding of STAT1 and STAT2. J Virol. 80(6)(2006):2675-2683.

Cenna J., Hunter M., Tan G.S., Papaneri A.B., Ribka E.P., Schnell M.J., Marx P.A., and McGettigan J.P. Replication-deficient rabies virus-based vaccines are safe and immunogenic in mice and nonhuman primates. J Infect Dis.200(8)(2009):1251-1260.

Etessami R, Conzelmann KK, Fadai-Ghotbi B, Natelson B, Tsiang H, Ceccaldi PE.

Spread and pathogenic characteristics of a G-deficient rabies virus

recombinant: an in vitro and in vivo study. J Gen Virol. 81(Pt 9)(2000):2147-2153.

Faber M., Pulmanausahakul R., Nagao K., Prosniak M., Rice A.B., Koprowski H., Schnell

M.J., and Dietzschold B. Identification of viral genomic elements responsible for

rabies virus neuroinvasiveness. Proc Natl Acad Sci U S A. 101(46)(2004):16328-

16332.

Faber M., Faber M.L., Li J., Preuss M.A., Schnell M.J., and Dietzschold B. Dominance of

a nonpathogenic glycoprotein gene over a pathogenic glycoprotein gene in

rabies virus. J Virol. 81(13)(2007):7041-7047.

Finke S., Cox J.H., and Conzelmann K.K. Differential transcription attenuation of rabies

virus genes by intergenic regions: generation of recombinant viruses

overexpressing the polymerase gene. J Virol. 74(16)(2000):7261-7269.

Finke S., Mueller-Waldeck R., and Conzelmann K.K. Rabies virus matrix protein

regulates the balance of virus transcription and replication. J Gen Virol. 84(Pt

6)(2003):1613-1621.

Graham SC, Assenberg R, Delmas O, Verma A, Gholami A, Talbi C, Owens RJ, Stuart

DI, Grimes JM, Bourhy H. Rhabdovirus matrix protein structures reveal a novel

mode of self-association. PLoS Pathog. 4(12)(2008):e1000251.

Grdzelishvili V.Z., Smallwood S., Tower D., Hall R.L., Hunt D.M., and Moyer S.A. A single

amino acid change in the L-polymerase protein of vesicular stomatitis virus

completely abolishes viral mRNA cap methylation. J Virol. 79(12)(2005):7327-

7337.

Grdzelishvili V.Z., Smallwood S., Tower D., Hall R.L., Hunt D.M., and Moyer S.A.

Identification of a new region in the vesicular stomatitis virus L polymerase

protein which is essential for mRNA cap methylation. Virology. 350(2)(2006):394-

405.

Hemachudha T., Laothamatas J., and Rupprecht C.E. Human rabies: a disease of

complex neuropathogenetic mechanisms and diagnostic challenges. Lancet

Neurol. 1(2)(2002):101-109.

Hwang, L. N., Englund, N., and Pattnaik, A. K. Polyadenylation of vesicular stomatitis

virus mRNA dictates efficient transcription termination at the intercistronic gene

junctions. J Virol. 72(3)(1998):1805-1813.

Ito N, Kakemizu M, Ito KA, Yamamoto A, Yoshida Y, Sugiyama M, Minamoto N. A

comparison of complete genome sequences of the attenuated RC-HL strain of

rabies virus used for production of animal vaccine in Japan, and the parental

Nishigahara strain. Microbiol Immunol. 45(1)(2001):51-58.

Ito N, Moseley GW, Blondel D, Shimizu K, Rowe CL, Ito Y, Masatani T, Nakagawa K,

Jans DA, Sugiyama M. Role of interferon antagonist activity of rabies virus

phosphoprotein in viral pathogenicity. J Virol. 84(13)(2010):6699-6710.

Javier R.T., and Rice A.P. Emerging Theme: Cellular PDZ Proteins as Common Targets

of Pathogenic Viruses. J Virol. 85(2011):11544-11556.

Lafon M, Mégret F, Meuth SG, Simon O, Velandia Romero ML, Lafage M, Chen L,

Alexopoulou L, Flavell RA, Prehaud C, Wiendl H. Detrimental contribution of the

immuno-inhibitor B7-H1 to rabies virus encephalitis. J Immunol.

180(11)(2008):7506-7515.

Lafon M. Evasive strategies in rabies virus infection. Adv Virus Res. 79(2011):33-53.

Masatani T., Ito N., Shimizu K., Ito Y., Nakagawa K., Sawaki Y., Koyama H., and

Sugiyama M. Rabies virus nucleoprotein functions to evade activation of the

RIG-I-mediated antiviral response. J Virol. 84(8)(2010):4002-4012.

Masatani T., Ito N., Shimizu K., Ito Y., Nakagawa K., Abe M., Yamaoka S., and Sugiyama

M. Amino acids at positions 273 and 394 in rabies virus nucleoprotein are

important for both evasion of host RIG-I-mediated antiviral response and

pathogenicity. Virus Res. 155(1)(2010):168-174.

Mavrakis M, Méhouas S, Réal E, Iseni F, Blondel D, Tordo N, Ruigrok RW.Rabies virus

chaperone: identification of the phosphoprotein peptide that keeps

nucleoprotein soluble and free from non-specific RNA. Virology. 349(2)(2006):422-429.

Mebatsion T., Weiland F., and Conzelmann K.K. Matrix protein of rabies virus is responsible for the assembly and budding of bullet-shaped particles and interacts with the transmembrane spike glycoprotein G. J Virol. 73(1)(1999):242-250.

Mebatsion T. Extensive attenuation of rabies virus by simultaneously modifying the dynein light chain binding site in the P protein and replacing Arg333 in the G protein. J Virol. 75(23)(2001):1496-1502.

Mita T., Shimizu K., Ito N., Yamada K., Ito Y., Sugiyama M., and Minamoto N. Amino acid at position 95 of the matrix protein is a cytopathic determinant of rabies virus. Virus Res. 137(1)(2008):33-39.

Morimoto K., Hooper D.C., Carbaugh H., Fu Z.F., Koprowski H., and Dietzschold B. Rabies virus quasispecies: implications for pathogenesis. Proc Natl Acad Sci U S A. 95(6)(1998):3152-3156.

Prehaud C., Wolff N., Terrien E., Lafage M., Megret F., Babault N., Cordier F., Tan G.S., Maitrepierre E., Menager P., Chopy D., Hoos S., England P., Delepierre M., Schnell M.J., Buc H., and Lafon M. Attenuation of rabies virulence: takeover by the cytoplasmic domain of its envelope protein. Sci Signal. 3(105)(2010):ra5.

Pulmanausahakul R., Li J., Schnell M.J., and Dietzschold B. The glycoprotein and the

matrix protein of rabies virus affect pathogenicity by regulating viral replication

and facilitating cell-to-cell spread. J Virol. 82(5)(2008):2330-2338.

Okumura A., and Harty R.N. Rabies virus assembly and budding. Adv Virus Res.

79(2011):23-32.

Sakamoto S., Ide T., Nakatake H., Tokiyoshi S., Yamamoto M., Kawai A., and Smith J.S.

Studies on the antigenicity and nucleotide sequence of the rabies virus

Nishigahara strain, a current seed strain used for dog vaccine production in

Japan. Virus Genes. 8(1)(1994):35-46.

Schnell M.J., and Conzelmann K.K. Polymerase activity of in vitro mutated rabies virus L

protein. Virology. 214(2)(1995):522-530.

Schnell MJ, McGettigan JP, Wirblich C, Papaneri A. The cell biology of rabies virus:

using stealth to reach the brain. Nat Rev Microbiol. 8(1)(2010):51-61.

Shimizu K, Ito N, Mita T, Yamada K, Hosokawa-Muto J, Sugiyama M, Minamoto N.

Involvement of nucleoprotein, phosphoprotein, and matrix protein genes of

rabies virus in virulence for adult mice. Virus Res. 123(2)(2007):154-160.

Shoji Y., Inoue S., Nakamichi K., Kurane I., Sakai T., and Morimoto K. Generation and

characterization of P gene-deficient rabies virus. Virology. 318(1)(2004):295-305.

Smallwood, S., Easson, C. D., Feller, J. A., Horikami, S. M., and Moyer, S. A. Mutations in

   conserved domain II of the large (L) subunit of the Sendai virus RNA polymerase

   abolish RNA synthesis. Virology. 262(2)(1999):375-383.

Stillman, E. A., and Whitt, M. A. Mutational analyses of the intergenic dinucleotide and

   the transcriptional start sequence of vesicular stomatitis virus (VSV) define

   sequences required for efficient termination and initiation of VSV transcripts. J

   Virol. 71(3)(1997):2127-2137.

Tang K. and Wu X. Computational analysis suggests that lyssavirus glycoprotein gene

   plays a minor role in viral adaptation. Int J Evol Biol.(2011):143498.

Vos A., Neubert A., Aylan O., Schuster P., Pommerening E., Muller T., and Chivatsi D.C.

   An update on safety studies of SAD B19 rabies virus vaccine in target and non-

   target species. Epidemiol Infect. 123(1)(1999):165-175.

Wang Z.W., Sarmento L., Wang Y., Li X.Q., Dhingra V., Tseggai T., Jiang B., and Fu Z.F.

   Attenuated rabies virus activates, while pathogenic rabies virus evades, the host

   innate immune responses in the central nervous system. J Virol.

   79(19)(2005):12554-12565.

Wirblich C., and Schnell M.J. Rabies virus (RV) glycoprotein expression levels are not

   critical for pathogenicity of RV. J Virol. 85(2)(2011):697-704.

Wunner W.H.. Rabies Virus. In: Jackson A., and Wunner W.H., eds. Rabies, 2nd edn.

   Elsevier, San Diego, CA., pp. 23-68; 2007

Wu X, Gong X, Foley HD, Schnell MJ, Fu ZF. Both viral transcription and replication are

reduced when the rabies virus nucleoprotein is not phosphorylated. J Virol.

76(9)(2002):4153-4161.

Wu X., and Rupprecht C.E. Glycoprotein gene relocation in rabies virus. Virus Res.

131(1)(2008):95-99.

Yamada K, Ito N, Takayama-Ito M, Sugiyama M, Minamoto N. Multigenic relation to the

attenuation of rabies virus. Microbiol Immunol. 50(1)(2006):25-32.

APPENDICES

APPENDIX A

Rabies Virus Titration in NA cells

1. Prepare confluent monolayers of NA cells in 24-well cell culture plate (Nunc, Thermo Scientific) 1 day before infection

2. Prepare serial 10-fold dilutions (10^{-1} to 10^{-7}) of virus in chilled maintenance medium, 2%DMEM (Dulbecco's Midified Eagle Media, DMEM, supplemented with 2% of fetal bovine serum, FBS)

3. Remove culture medium and add 200ul of virus inoculums, starting from the highest dilution. Ensure that a film of medium completely covers the cell surface

4. Incubate the plate at 37°C for 1 hour with intermittent rocking of the plate

5. Remove the inoculums completely with a pipette and then add 1ml of fresh medium , 2%DMEM and incubate at 37°C for 48 hours post inoculation

6. Remove culture medium

7. Fix the cells by adding 2ml of 90% freshly prepared acetone. Wait for 3 minutes then remove acetone and wait until cells dry completely

8. Stain the cells by adding 150ul of FITC Anti-Rabies Monoclonal Globulin (Fujirebio Diagnostics, Inc) to each well. Incubate plate at 37°C for 1 hour with intermittent rocking of the plate then wash the cells twice with phosphate buffer saline (PBS) pH7.2 and wait until cells dried completely

9. Count 30 fields per well using immunofluorescent microscopy with 20x objective

   lens. At least one infected cell was considered as the infected field.

10. Calculate median tissue culture infectious dose.

APPENDIX B

TA cloning of G gene into pGEM-T ® easy vector

1. Polymerase chain reaction was performed to obtain G1.2 and G1.5 PCR fragments as described above with primers RabG1.2a and RabG1.2b, and RabG1.5a and RabG1.5b, respectively. The second round PCR was performed using pooled PCR products of G1.2 and G1.5 as template with RabG1.2a and RabG1.5b primers.

2. Agarose gel electroporesis and gel extraction using Nucleospin® Extract II (Macherey-Nagel, USA) then elute DNA with 15ul of TE buffer pH 8.0

3. Addition of A tail to PCR products using 10x A-Attachment mix (TOYOBO, Japan)

4. Ligation of A-tailed PCR products to pGEM-T®easy vector using ligation mix, (TaKaRa, Japan)

   1) Dilute pGEM-T®easy vector1:10 in TE Buffer resulting to 5ng/µl

   2) Prepare Ligation reaction by adding 1:10 pGEM-T easy vector, 6ul of A-tailed PCR product and 7ul of ligation mix to 200ul thin-wall tube

   3) Put ligation reaction into thermocycler at 16°C at least 1 hour

4) Transfer ligation reaction to 0.6ml microcentrifuge tube just before starting

transformation

5. Transformation

1) Thaw XL10-Gold on ice and transfer50 µl of thawed XL10-Gold to ligation

reaction then mix by pipetting gently 3 times and keep on ice 3 minutes

2) Heat shock using water bath at 42°C for 45 seconds and keep on ice for 3

minutes

3) Transfer to 1 ml of Luria-Bertani (LB) broth and mix well

4) Spread 20 µl of 50mg/ml 5-bromo-4-chloro-3-indolyl-beta-D-

galactopyranoside (X-Gal) and 30 µl of 100mM isopropyl thiogalactoside (IPTG)

on LB agar plate containing 50mg/ml of ampicillin then incubate in air incubator

at 37°C for 1 hour or until the surface dried

5) Spread 150 µl of LB/E.coli mix on 4) and incubate in air incubator at 37°C for

12-16 hours

6) Collect plates and store at 4°C for 2-3 hours for colonies to completely

develop blue color

8) Count blue and white colonies on plate; the numbers of white colonies should

be at least twice the number of blue colonies

6. Plasmid Extraction using Nucleospin® Plasmid (Macherey-Nagel, USA)

1) Prepare LB broth containing 50mg/ml of ampicillin by adding 5ul of 100mg/ml of ampicillin to 10 ml of LB broth (in 50ml conical tube)

2) Pick a single white colony by using autoclaved micropipette tip and drop the tip into 1)

3) Shake the tube in shaking incubator at 37°C 200rpm for 16 hours; do not exceed 18 hours to avoid shearing of plasmids

4) Transfer to 15ml conical tube and centrifuge at 3000rpm 4°C for 20minutes then discard supernatant

5) Extract pellet using Nucleospin® Plasmid (Macherey-Nagel, USA) according to manufacturer's protocol and elute with 55ul of nuclease-free water

6) Aliquot 4ul of extracted plasmid to 0.6ml microcentrifuge tube and check the quality and quantity by electrophoresis 1ul and Nanodrop measurement, respectively

7) Sequencing extracted plasmids.

BIOGRAPHY

Miss Phatthamon Virojanapirom was born in Bangkok, Thailand in Jane 15th, 1984. In 2006, she received her bachelor degree (first class honor) in Medical Technology from Faculty of Allied Health Science, Chulalongkorn University.